# PARAMETRIC STUDY OF METAL SEMICONDUCTOR FIELD EFFECT TRANSISTOR (MESFET)

by

**ASHADUR RAHAMAN**

Examination Roll No.: M6VLS22013
Registration No.: 150141 of 2019-2020

*A comprehensive project report submitted in partial fulfillment of the requirement for the degree of*

**MASTER OF TECHNOLOGY**

in

**VLSI DESIGN AND MICRO ELECTRONICS TECHNOLOGY**

*Under the supervision of*

**Dr. MANOTOSH BISWAS**

Professor

Department of
Electronics & Telecommunication Engineering

Jadavpur university
Kolkata – 700032

August - 2022

# FACULTY OF ENGINEERING AND TECHNOLOGY
# JADAVPUR UNIVERSITY

## CERTIFICATE OF EXAMINATION

This is to certify that the thesis entitled "**Parametric Study of Metal–Semiconductor Field Effect Transistor (MESFET)"** carried out by **Ashadur Rahaman** (Examination Roll No. M6VLS22013, Registration No. 150141 of 2019-2020) under my guidence and supervision, be accepted in partial fulfillment of the requirements for the award of the degree of Master of Technology in VLSI Design and Microelectronics Technology. To the best of my knowledge, the matter embodied in the thesis has not been submitted for the award of any degree to any other University or Institute.

**……..….**

**(Prof. Manotosh Biswas)**

Supervisor

Department of Electronics & Telecommunication Engineering

Jadavpur University

Kolkata – 700032

**……..**

**(Prof. Manotosh Biswas)**

Head of the Department

Department of Electronics &

Telecommunication Engineering

Jadavpur University

Kolkata – 700032

**……..….**

**(Prof. Chandan Mazumdar)**

Dean

Faculty Council of Engineering and

Technology (FET)

Jadavpur University

Kolkata – 700032

# FACULTY OF ENGINEERING AND TECHNOLOGY
# JADAVPUR UNIVERSITY

## *CERTIFICATE OF APPROVAL**

This is to certify that the Master of Technology thesis entitled "**Parametric Study of Metal–Semiconductor Field-Effect Transistor (MESFET)"** is hereby approved as a creditable study of an engineering subject, carried out and presented in a manner satisfactory to warrant its acceptance as a pre-requisite to the degree for which it has been submitted. It is understood that by this approval the undersigned do not necessarily endorse or approve every statement made, opinion expressed, or conclusion drawn therein but approve the thesis only for the purpose for which it has been submitted.

Committee on final examination for the evaluation of thesis of:

**ASHADUR RAHAMAN**

Examination Roll No.: M6VLS22013

Registration No.: 150141 of 2019-2020

……..

Signature of Supervisor

…….

Signature of Examiner

*Only in case the thesis is approved

# FACULTY OF ENGINEERING AND TECHNOLOGY
# JADAVPUR UNIVERSITY

## *DECLARATION OF ORIGINALITY AND COMPILANCE OF ACADEMIC ETHICS*

I hereby declare that the M. Tech thesis submitted to the Faculty of Engineering and Technology , Jadavpur University as a part of fulfillment of degree of Master of Technology in VLSI Design and Microelectronics Technology, is an original work carries out by undersigned. All information in this document have been obtained and presented in accordance with academic rules and ethical conduct. The matter embodied in this project is genuine work done by the undersigned and has not submitted to any other University/Institute for the fulfillment of the requirement of any course of study.

I also declare that, as required by these rules and conduct, I have fully cited and referenced all material and results that are not original to this work.

| | |
|---|---|
| Name of the Candidate: | **ASHADUR RAHAMAN** |
| Examination Roll No.: | M6VLS22013 |
| Registration No.: | 150141 of 2019-2020 |
| Department: | Electronics and Tele Communication Engineering |
| Signature of the Candidate: | |
| Date: | ……. |

# *ACKNOWLEDGEMENT*

*I humbly praise and grateful to ALMIGHTY ALLAH, who permits me to live and accomplish tasks including the research work being presented in this thesis.*

*I would like to express my sincere graduate to my supervisor, Professor and Head of the Department Dr. Manotosh Biswas for his valuable guidance and insightful suggestions throughout my thesis work. I am very much indebted to his for giving me the opportunity to pursue my M. Tech thesis work under his guidance. Without his precious knowledge and exceptional encouragement my project work would not have taken a meaningful shape. I will be benefited throughout my life from the knowledge, rightful guidance and unparallel professionalism that I acquired here.*

*Besides, I would also like to thank all Faculty members of our esteemed department for their constant support, cooperation, motivation, provided me during the different phase of building the aforesaid project which served as a constant source of inspiration presence and blessings.*

*I would also like to thank all Staff members of Electronics and Tele Communication Engineering Department for providing me a friendly environment and facilities to complete this thesis.*

*I would like to thank Mr. Biplab Biswas, Ms. Baisakhi Naskar , Mr Sheershendu Bhattacharya. Ph.D student of Jadavpur University for their help, criticisms and suggestions which helps me to complete this thesis.*

*I would specially like to thank our all my friends, classmates for their support and encouragements.*

*I also wish to express my feeling of gratitude to my parents, who prayed for my health and brilliant future. I am grateful to my beloved wife and children, Safika Parveen and Arfan Imroze for supporting me during this extremely exhaustive period of research. I would not have achieved the goals without their sincere co-operation and love.*

# ABSTRACT

MESFETs (Metal Semiconductor Field Effect Transistor) are usually fabricated in compound semiconductor (Group III-V, Group IV-IV) technologies lacking high quality surface passivation such as gallium arsenide (GaAs), indium phosphide (InP), or silicon carbide (SiC), and are faster but more expensive than silicon-based Junction Field Effect Transistors (JFET) or Metal Oxide Silicon Field Effect Transistors (MOSFET). The gallium arsenide (GaAs) having electron mobility six times higher than silicon (Si). It became an essential instrument in modern electronics as well because of its inherent properties such as high temperature conductivity, very low intrinsic concentration, high frequency, higher band-gap, higher electric field strength breakdown.

The MESFETS are the most active components used in microwave communication system. To achievement the better performance of these components' circuits, it become necessary to develop techniques for high end numerical simulation based on physical and structural mechanisms that govern the operation of these devices and circuits. The properties of MESFET could be determined from an original analytical study based on the resolution of the semiconductor fundamental equations.

This thesis analyze several parameters of MESFET such as, Drain-Source Current as a function of Drain-Source Voltage, Transconductance as a function Gate-Source Voltage, , Variation of Gate-Drain Capacitance with Drain-Source Voltage, Variation of Gate-Source Capacitance with Respect to Gate-Source Voltage, Variation of Total Internal Device Capacitance with Gate Length and Modelling of MESFET DC Characteristics in different Temperature using Finite Element Analysis Software COMSOL Multi Physics.

# Contents

# LIST of Table



# List of Figure

# Chapter 1: Introduction

In the innovative years of electronics i.e., before the 1940s, electron tubes were commonly used in the electronic systems, such as radio and television, but they had some serious limitations pertaining to their performance. Then a better discovery was made in 1947, when Bardeen and Brattain invented the transistor by using a slice of germanium with a few carefully placed wires [Brattain-1947]. Since its inception, the transistor brought a revolution to the industry and in day-to-day life through its use in automation, control and communication equipment. The diverse industrial demand eventually led to different types of transistors currently available in the market.

The concept of Schottky barrier FET was introduced by Schottky [Schottky- 1938]. He gave the idea of formation of a potential barrier due to the difference of work function between the metal and the semiconductor contacts. After a researcher from Bell Laboratories William Shockley [Schockley-1948] invented the junction transistor and Bell Laboratories announced this invention in 1951. Schottky's idea was utilized by Mead in 1966 for the fabrication of Metal Semiconductor Field Effect Transistor (MESFET) [Mead-1966] and subsequently it was fabricated by Hooper in 1967 using a Gallium Arsenide (GaAs) epitaxial layer on semi-insulating GaAs substrate [Hooper-1967]. A MESFET is a three-terminal device like any other transistor [Sze-1985, Soares-1988]. These terminals are named as Source, Drain and Gate as shown in Figure (1.1) Charge carriers (electrons) flow from the source to the drain via a channel. The channel is defined by doping the epitaxial layer grown on semiconductor and offers good conduction. The flow of charge carriers in the channel is controlled by a Schottky barrier gate. The main advantages of a MESFET compared to its counter parts are:

(a) high electron velocity inside the channel;

(b) smaller transit time leading to faster response and

(c) fabrication of active layer on semi-insulating GaAs substrates to decrease the parasitic capacitances.

In 1970, for microwave applications, Middlehoek realizes that Silicon based MESFETs with 1 μm gate length had maximum oscillation frequency up to 12 GHz [Middlehoek-1970]. In 1971, Turner took a step, when 1 μm gate length FETs were made on GaAs with maximum frequency

upto 50 GHz [Turner-1971]. Such a high performance is attributed to GaAs which offers superior electrical properties compared to the Silicon. Beside high frequency of oscillation GaAs MESFETs also provide high output power with low noise figure. Owing to these attributes GaAs MESFETs are overwhelmingly used in microwave integrated circuits [Ladbrooke- 1991, Golio-1991, Bose-2001 and Khalaf-2000].

GaAs MESFETs have demonstrated excellent noise and gain performance at microwave frequency and they are used quite often in pre-amplifiers of communication devices. In today's world, high frequency communication is possible because of the superior electrical properties offered by GaAs MESFETs both in analog as well as in digital applications. A properly designed GaAs MESFET can operate comfortably at a frequency higher than 100 GHz [Ahmed-2003]. Whereas, a High Electron Mobility Transistor (HEMT) of submicron gate length can operate higher than 900 GHz [Das-1987 and Cidronali-2003]. An excellent microwave performance of a GaAs MESFET is certainly related to its channel properties [Golio-1991]. For low noise applications, there are special constraints on the design of a MESFET to achieve target performance [Fukui-1979, Feng-1992 and Hung-1988].

## 1.1 MESFET Operation

The MESFET has three terminals i.e., Gate, Source and Drain. Below the conduction channel it has a semi-insulating substrate layer. The n-doped region acts as the channel for carrier flow, can be formed in two ways: (i) by ion implantation technique or (ii) by growing an epitaxial layer. Ion implantation technique involves ion diffusion in the lightly n-doped layer. Epitaxial growth is a process where crystals are grown in a particular orientation over another crystal. It can be of two kinds. The process is called Homoepitaxy if both crystals are of the same material, and another is known as heteroepitaxy if the materials are different. On both sides of the n-doped channel an n+ doped region is implanted which works as Source and Drain of the MESFET. Thus, three distinct terminals of a MESFET are formed by placing metal contacts on the top of the Gate, Source and Drain. The gate metal contact and n-doped semiconductor material junction created a Schottky barrier junction.

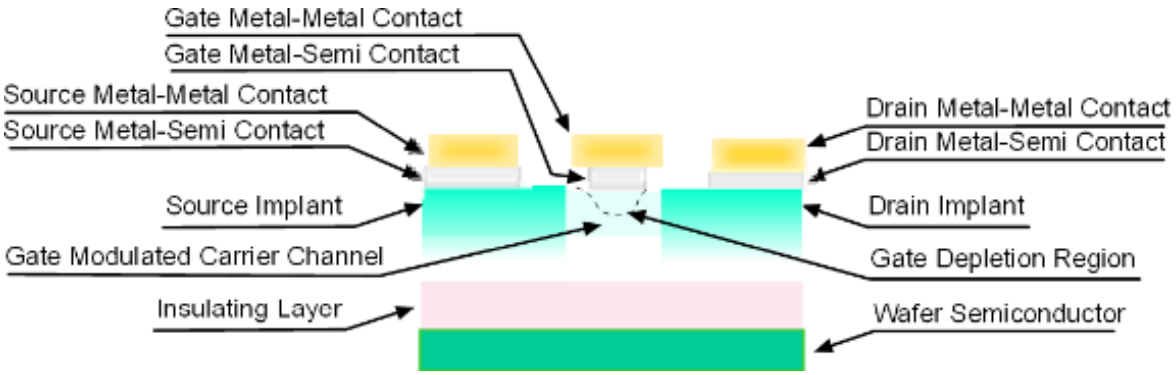


**Figure 1-1Basic MESFET structure**

## 1.2 Types of MESFET

Two types of MESFET are there: Depletion type MESFET and Enhancement type MESFET.

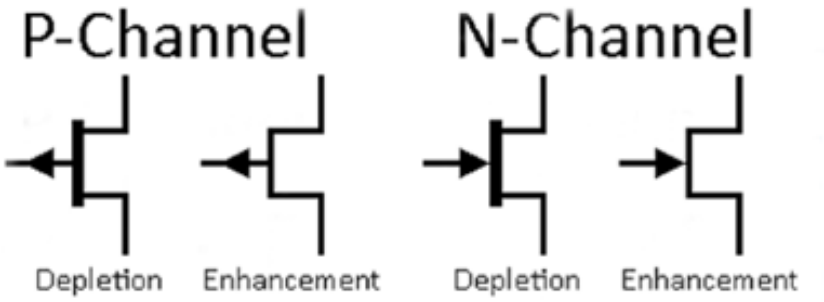


**Figure 1-2 MESFET Symbol**

### 1.2.1 Depletion type MESFET

The depletion width of n-channel MESFET (Figure1.2.1) is varied by changing applied gate voltage at gate terminal. By applying a negative voltage at the gate-to-source terminals causes the depletion width to increases and make the channel width narrower, obstructing the flow of carriers. The junction between gate and channel thus becomes reverse biased. If the depletion layer is expended more and more then after a certain time it will completely block the channel or pinches-off` the channel, the resistance of the channel from source to drain becomes large, causing the MESFET to be turned off. Here MESFET works like a switch.

After applying a positive gate-to-source voltage will cause the depletion layer to minimize allowing the channel size to increase again turning the MESFET on.

### 1.2.2 Enhancement type MESFET

In n-channel Enhancement type MESFET the channel is completely blocked by the depletion region naturally. Therefore, the MESFET is switch off mode as shown Figure 1.2.2. To enable the device in conduction mode the barrier needs to be reduced so that the channel become expended and carrier can flow. Narrowing the barrier/depletion layer can be done by gate biasing. This can be achieved by applying a positive voltage at the gate terminal. By doing this the junction become forward biased. As the width of channel increases the carrier starts flowing and the device becomes in conduction mode.

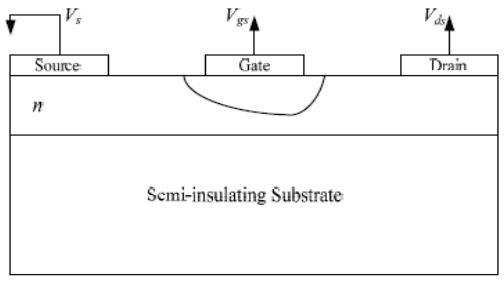


**Figure 1-3 Depletion type MESFET**

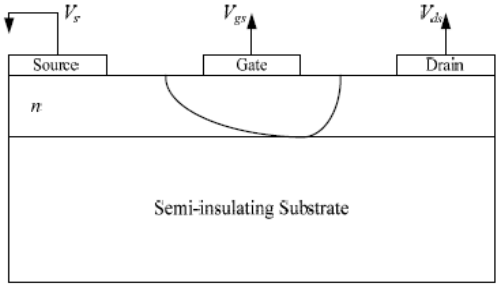


**Figure 1-4 Enhancement type MESFET**

## 1.3 Principle of MESFET Operation:

Biasing of the device can be achieved by Drain to source voltage $(V_{DS})$ and Gate to source Voltage $(V_{GS})$. These two voltages control the line current Ids by changing the longitudinal electric field and also varying the depth of gate depletion region. The IV characteristics of a MESFET are shown in the figure1.5. Here The drain current $(I_{DS})$ is plotted as a function of drain-source voltage $(V_{DS})$. The drain current is also a function of gate-source voltage$(V_{gs})$. An individual curve in the figure represents the dependency of drain current $(I_{Ds})$ in drain-source

voltage ($V_{DS}$) for a particular value of gate-source voltage ($V_{GS}$). Another mode of MESFET operation is known as breakdown mode where excessive drain-source voltage is applied.

Necessary voltage should be given in the gate electrode to operate the MESFET in depletion mode. Applying more negative voltage in the gate terminal makes the junction more reversed biased which results in increase of depletion region. If negative voltage I the gate terminal keep increasing the channel will gates entirely depleted, therefore no current flows. The voltage that makes the doped channel layer fully depleted called the Threshold voltage of the MESFET. Figure 1.5 yields that the value of $I_D$ is very low for lower $V_{GS}$. More increase of the negative voltage in gate terminal will stop the channel. Therefore, we can say that the threshold voltage of the figure1.5 is near the lowest $V_{GS}$ curve. It can be said that current conducting region are $V_{GS} > V_T$. Threshold voltage is denoted by $V_T$.
A short description of different region of operation of MESFET is given below.

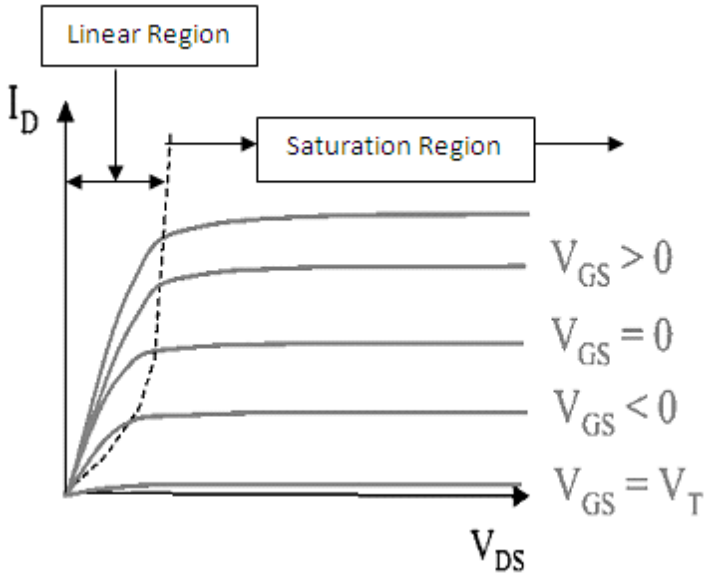


**Figure 1-5 I-V characteristics curve**

**Liner Region($0 < V_{DS} < V_{DSat}$ ):**

MESFET operated in this region when the value of $V_{DS}$ is low. As shown in the figure 1.3.1 that when value of $V_{DS}$ is low the drain current $I_{DS}$ varies linearly on $V_{DS}$ for a particular value of

$V_{GS}$. As current varies linearly so the region is called linear region. It is also known as triode region. MESFET operated in this region only when $V_{DS} < V_{DSat}$ where
$V_{DSat} = V_{GS} - V_{TO}$

**Saturation Region ($V_{DS} > V_{DSat}$):**

It is discussed above in the linear region that when $I_D$ increases with the increases of $V_{DS}$ . But after a certain time $I_D$ does not change significantly with the increases of $V_{DS}$. Saturation of $I_D$ is reached when $V_{DS} = V_{DSat}$. The pinch off point shift from drain to source results this phenomenon. This pinch off phenomena eventually decreases the channel length. Saturation may occur in two different ways as discussed below.

## 1.4 MESFET operation under different biasing condition.

### 1.4.1 (i)Saturation by pinch off:

The MESFET fabricated by material like Si which has high saturation electric filed achieved saturation by pinching off the channel between the source and drain. Having high saturation electric field value, the drift velocity of the carrier saturates at higher value of the electric field along the channel. Here the mobility is considered as a constant throughout the process and the depletion in the drain side increases with the increases value of $V_{DS}$ . After a certain value of $V_{DS}$ the drain side depletion pinch of the channel. In this situation the channel impedance is high and no carrier can pass through the channel. But at high electric field some of the carrier may swept off to the drain side and thus the saturation current. The pinch off occur while $V_{DS} > V_{DSat}$

### 1.4.2 (ii) Saturation by velocity

In the material like GaAs the drift velocity of the carrier saturates completely at lower electric filed. The electric field is increases by applying higher $V_{DS}$ beyond the saturation. The high electric field saturated the carrier velocity through the channel. This device has short channel because it ensure the good strength of electric field which is desirable. The saturation in the drain current $I_{DS}$ occurs due to the velocity saturation of the carrier.

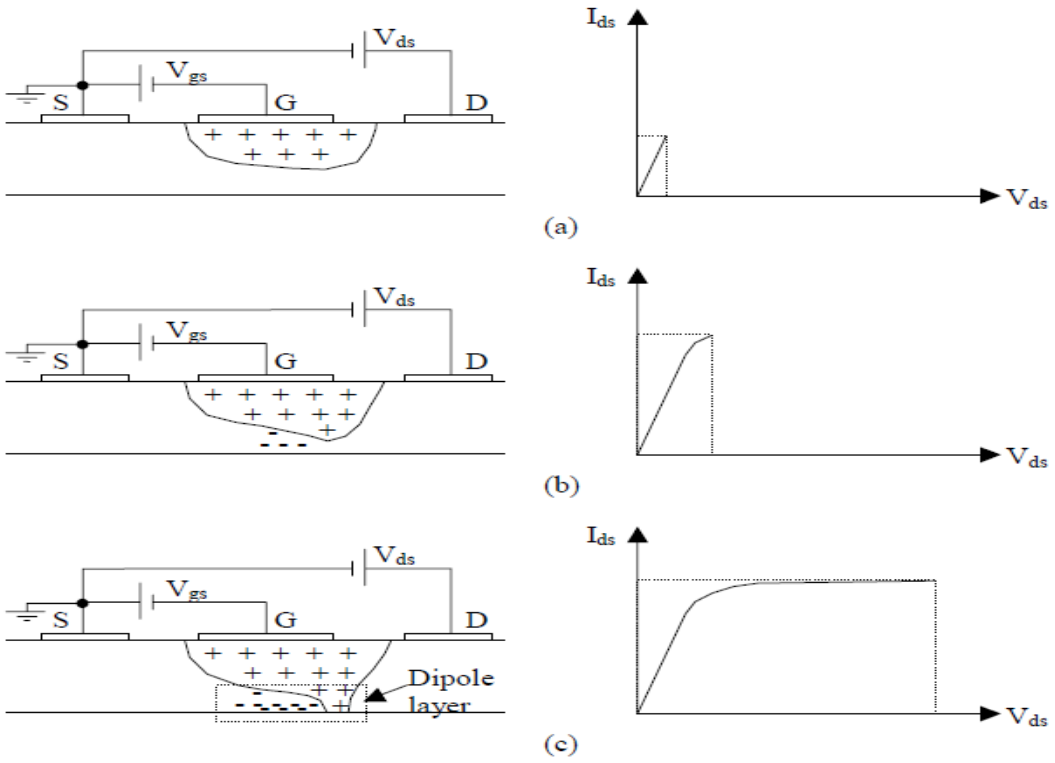


**Figure 1-6 Vds biasing with Vgs = 0: a) Linear region (Vds low), b) Vds at the commencement of saturation, c) Vds big**

## 1.5 Structure of MESFET

The structure of the mesfet is of two kinds (i) self align self aligned source and drain MESFET and (ii) non self aligned source and drain MESFET.

The short description of the abobe is given below.

### 1.5.1 (i) Self-aligned source and drain

In this form of structure, the gate contact covers the whole length and reduces the channel length. This can be done by forming the gate first. The annihilating process required after the formation of the source and drain area by ion implantation. The gate contact must be able to withstand the high temperature. A limited number of materials being suitable to fabricate this structure.

### 1.5.2 (ii) Non-self aligned source and drain

In non-self aligned form the gate is placed on a portion of the channel. The gate contact does not cover the entire length of the channel. Here source and drain contact are normally formed before the gate.

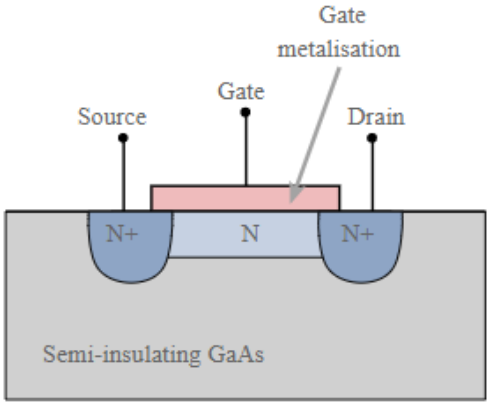


**Figure 1-7 Self-aligned MESFET**

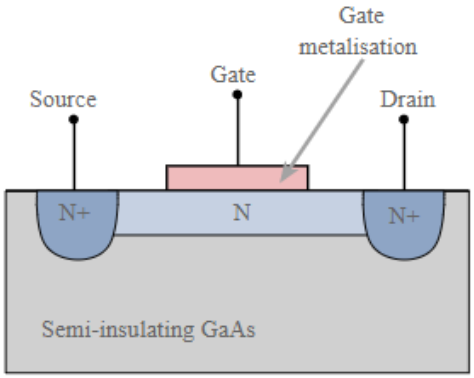


**Figure 1-8 non-self-aligned MESFET**

## 1.6 Microwave MESFET's Equivalent Circuit

The equivalent circuit depends upon the physical construction of the device. The cross-sectional view of a GaAs MESFET is shown in figure 1.5 showing the origin of device electrical components.

The circuit elements in this figure are:

drain-pad capacitance, ($C_{pd}$); source resistance ($R_s$); drain inductance, ($L_d$); gate resistance ($R_g$); drain resistance ($R_d$); gate-source capacitance ($C_{gs}$); channel resistance ($R_i$); contact resistance ($R_c$); source inductance ( $L_s$); gate inductance ($L_g$); gate-drain capacitance ($C_{gd}$); gate-pad capacitance, ($C_{pg}$); and drain-source capacitance ($C_{ds}$);

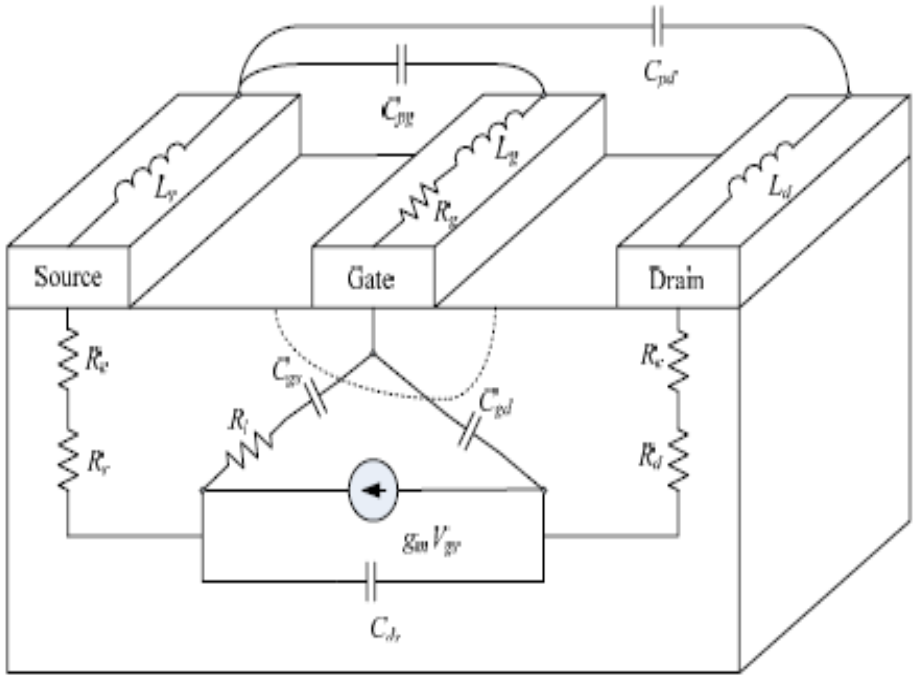


**Figure 1-9 A cross-sectional view of a GaAs MESFET showing the origin of device**

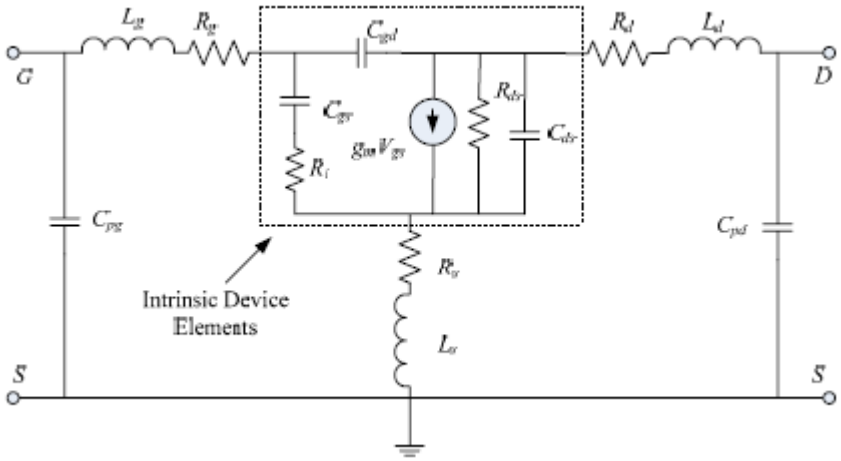


**Figure 1-10 small signal equivalent circuit of MESFET's in the saturation region of operation**

## 1.7 Application of MESFET

The MESFET has the characteristics of High electron mobility, Low capacititance levels, high input impedence, negative temperature coefficient, lack of oxide trap and high level of geometry control.

The high carrier mobility along with lower level of stray capacitance of MESFET make it useful for RF amplifier application, High frequency low noise amplifier, oscilator, broadbrand amplifier and microwave power amplifier.

For switching application MESFET schottky barrier diode is used.

Various biomedical and optolelectronics device are made of MESFET.

Due ti its shorter gate length, MESFET is widely used in high frequency communication like sattelite, radar, mobile communication.

# Chapter 2: Motivation

## 2.1 Factors of Motivation

Some important properties of GaN made it very useful for high power and microwave frequency applications. Some advantages of GaN over other materials are as follows:

• GaN has higher mobility compared to other materials such as SiC and Si which makes it the best material for very high frequencies.
• Almost the entire visible range of wavelengths is spanned in the Group III nitride alloy system. The band gap of nitride-based materials ranges from 1.9eV to 6.2eV.
• GaN possesses low dielectric constants and high thermal conductivity pathways.
• GaN has high bond strengths and very high melting temperatures. These high bond strengths improve its reliability compared to other materials.
• The nitrides are resistant to chemical etching and allow GaN based devices to be operated in harsh environments.
• GaN light sources will be compact and highly reliable and could result in enormous cost savings compared to conventional light sources.
• The use of GaN based LEDs may result in reduction of greenhouse gases and minimize the risk of global warming.
• Large application of GaN is in fabricating blue laser diodes for extremely high density optical storage systems [3].

## 2.2 Comparison Between GaAs, SiC and GaN

Table 2.1 shows the comparison between SiC, GaAs and GaN.

## 2.3 More on GaN and SiC FETs

SiC MESFETs and GaN HEMTs have an enormous potential in high-power amplifiers at microwave frequencies due to their wide bandgap features of high electric breakdown field

strength, high electron saturation velocity and high operating temperature. The high-power density combined with the comparably high impedance attainable by these devices also offers new possibilities for wideband power microwave systems.

**Table 2-1 Comparison between SiC, GaAs and GaN.**

| Material Property | SiC | GaAs | GaN |
|---|---|---|---|
| Band gap (eV) [4] | 3.2 | 1.43 | 3.4 |
| Electron Mobility ($cm^2$/V-sec)[5] | 900 | 8500 | 2000 |
| Electron Saturation Velocity ($10^6$ cm/sec)[6] | 22 | 12 | 25 |
| Thermal Conductivity (Watts/cm K) [7] | 5 | 0.5 | 1.3 |
| High/Low Power Device [8] | High | Low | High |

## 2.4 Wide Bandgap SiC and GaN Transistors

The fundamental physical limitations of Si operation at higher temperature and powers are the strongest motivations for switching to wide bandgap semiconductors such as SiC and GaN for these applications. For phase array radars, wireless communication market and other traditional military applications require demanding performance of microwave transistors. In several applications, as well as in radar and military systems, the development of circuits and sub-systems with broadband capabilities is required. From transmitter point of view the bottleneck, and the critical key factor, is the development of high-performance PA.

Next generation cell phones require wider bandwidth and improved efficiency. The development of satellite communications and TV broadcasting requires amplifiers operating both at higher frequencies and higher power to reduce the antenna size of terminal users. The same requirement holds for broadband wireless internet connections as well. This high power and high frequency applications require transistors with high breakdown voltage, high electron velocity and high thermal conductivity.

The wide band gap materials, like GaN and SiC are preferable as we can see from Table 2.2.

The high output power density of WBG transistors allows the fabrication of smaller size devices with the same output power. The operation at high voltage due to its high breakdown electric field not only reduces the need for voltage conversion, but also provides the potential to obtain high efficiency. The wide bandgap enables it to operate at elevated temperatures.

**Table 2-2 Material parameters of SiC and GaN compared to GaAs and Si [9].**

| Material | Bandgap [eV] | Critical electric field [MV/cm] | Thermal conductivity [W/cm-K] | Electron mobility [cm2/Vs] | Saturated electron drift velocity [cm/s] | Relative dielectric constant |
|---|---|---|---|---|---|---|
| 4H-SiC | 3.26 | 2 | 4.5 | 700 | $2x10^{7}$ | 10 |
| GaN | 3.49 | 3.3 | 1.7 | 900 | $1.5x10^{7}$ | 9 |
| GaAs | 1.42 | 0.4 | 0.5 | 8500 | $1 x10^{7}$ | 12.8 |
| Si | 1.1 | 0.3 | 1.5 | 1500 | $1 x10^{7}$ | 11.8 |

These attractive features in power amplifier enabled by the superior properties make these devices promising candidates for microwave power applications.

The critical electric field is the maximum field that the material can sustain before the onset of breakdown and is closely related to bandgap. When the electric field is so high that the carriers can acquire a kinetic energy larger than the band gap, new electron-hole pairs can be created through impact ionization. These newly created carriers are in turn accelerated and, if the electric field is sufficiently high the process is repeated again and again. This causes an increase in the current that will degrade the efficiency and output power and ultimately destroy the device due to the heat generated. Therefore the critical field limits the supply voltage that can be used for the transistor and hence output power.

The maximum current in the device under high electric field is controlled by the saturated electron velocity (by limiting the flux of electrons). A higher Vsat will allow higher current and hence higher power. SiC and GaN has higher Vsat compared to Si and GaAs according to Table 2.2

The electron mobility of SiC and GaN is inferior to that of Si and GaAs. This reduces the efficiency of the device by increasing the knee voltage especially in the case of SiC MESFET

but this effect is reduced by the high breakdown voltage of SiC, which enables a sufficiently high supply voltage that the knee voltage becomes small in comparison. The relatively low mobility of SiC also reduces the high frequency capability of devices. But the impact of the low mobility of SiC on the high frequency performance is partially offset by the high *Vsat*. Due to higher mobility and the ability to use high electron mobility transistor (HEMT) structures, GaAs and GaN transistors can be used at substantially higher frequencies than Si or SiC transistors.

Heat removal is a critical issue in microwave power transistors especially for class-A power amplifier operation and continuous wave (CW) applications. The thermal conductivity of SiC is substantially higher than that of GaAs and Si. The large bandgap and high temperature stability of SiC and GaN also makes them possible to operate devices at very high temperatures. At temperatures above $300^{0}$C, SiC and GaN have much lower intrinsic carrier concentrations than Si and GaAs. This implies that devices designed for high temperatures and powers should be fabricated from wide bandgap semiconductors, to avoid effects of thermally generated carriers. The higher impedance (higher supply voltage) and lower relative dielectric constant (reduces parasitic capacitances) for both SiC and GaN compared to Si and GaAs simplifies broadband.

impedance matching. Another important property of amplifiers is their linearity. Excellent linearity has been reported for SiC MESFETs both in power amplifiers and low noise amplifiers

# Chapter 3: Literature Review

## 3.1 Effect of Mobility on (I-V) Characteristics of GaAs MESFET

This paper presented an analytical model of the current–voltage (I-V) characteristics for submicron GaAs MESFET transistors. This model takes into account the analysis of the charge distribution in the active region and incorporate a field depended electron mobility, velocity saturation and charge build-up in the channel.

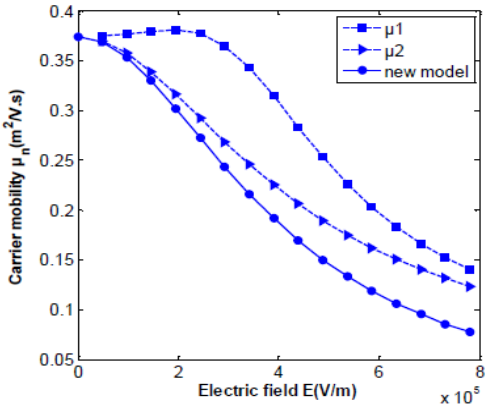


Figure 2. Comparison of the Experimental Results and Theoretical Modeling of Carrier Mobility for Submicron Gaas MESFET's as a Function of the Applied Electric

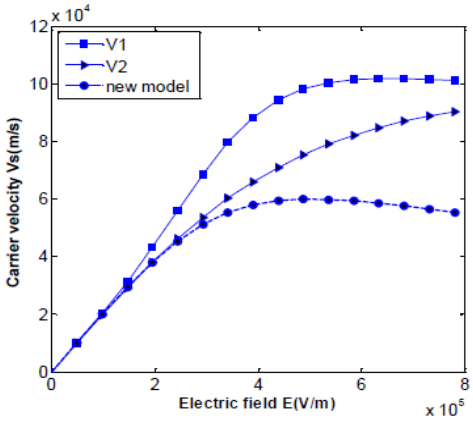


Figure 3. Comparison of the Experimental Results and Theoretical Modeling of Carrier Velocity for Submicron Gaas MESFET's as a Function of the Applied Electric

Figure 4 shows that the simulated drain current using the new model and measured I-V characteristics are in good agreement in different device operation regions, especially the linear and knee regions that are difficult to model. The modeled drain current goes smoothly to zero when Vgs approaches pinch-off. The new model also gives an accurate pinch off modeling, as indicated in Figure 5 which shows the comparison of measured and modeled drain current characteristics in pinch off region.

The RMS errors of the model are calculated and listed in Table 2. The calculation is made at four bias levels for Vgs, while Vds changes from 0.5V to 3.0V. Table 2 shows the RMS error is insignificant and greatly reduced near pinch off condition, the new model produces very accurate fitting result.

**Table 2. RMS Errors of the New Model at different Vgs Values**

| Vgs(V) | 0 | -1.1 | -2.2 | -3.3 |
|---|---|---|---|---|
| RMS Error (%) | 0.977 | 1.658 | 0.337 | 0.196 |

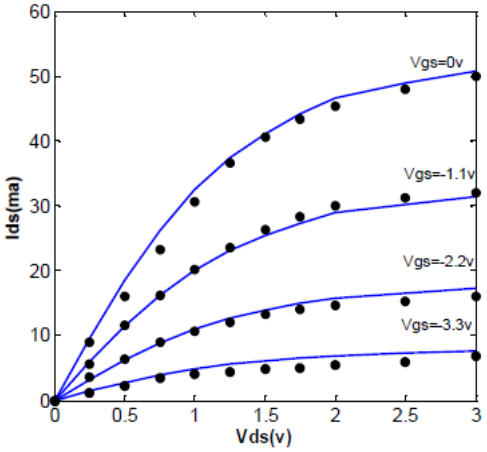


Figure 4. Measured Drain Current Characteristics Ids-Vds of GaAs [dot] and Comparison to Improved Model with a New Mobility Profile as a Fitting Parameter [Solid Line]

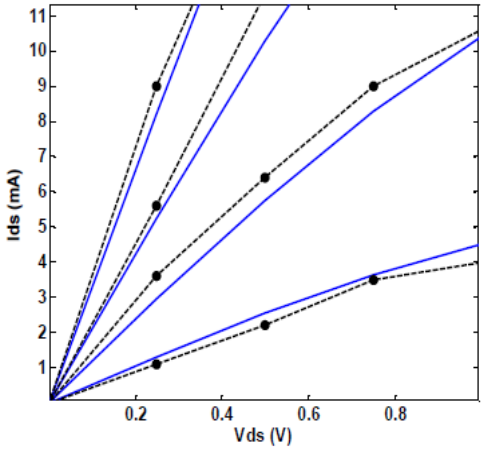


Figure 5. Comparison of measured [dot] and Modeled [Solid Line] Drain Current Characteristics near pinch off Region

The carrier mobility acquires major importance in determining the output characteristics of a GaAs MESFET's. A good fitting of mobility has a great influence on the accuracy of the electrical conductivity and many other physical parameters. This model also may be used in analytical calculations of the device performance (for example, when an analytical expression for the differential mobility as a function of the field is needed).

## 3.2 Determination of Characteristics and Performance Appraisal of GaN MESFET

This research article examines several properties such as intrinsic delay, gate to source capacitance, gate to drain capacitance, transconductance, cutoff frequency, and channel current for gallium nitride metal–semiconductor field-effect transistor as well as investigates the impact of variation in gate to source voltage on the channel current with proper evaluation of respective characteristics curves.

The main issues addressed in this article are a) observation of the channel current through the GaN MESFET, b) determination of parasitic capacitance such as gate to source capacitance and

gate to drain capacitance, c) assessment of transconductance, d) calculation of intrinsic gate delay, and e) finding the cutoff frequency with the variation of gate to source voltage in each case for a GaN-based MESFET.

The depletion region widens for the increase in negative gate to source voltage in contrast to the positive one the response of gate to source capacitance have been evaluated as outlined in Fig. 3, in the same way, it has been done for gate to drain capacitance. On the contrary to the previous characteristics, in this case, the gate to source capacitance rises with the increase in gate to source voltage and the slope of each characteristic curve is sharper as well with respect to the preceding ones. The reason behind the dissimilarities is the application of positive gate to source voltages.

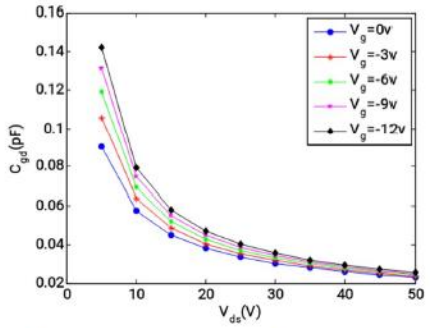


Fig. 2. The relationship between gate to drain capacitance (pF) and drain to source voltage (V) in GaN MESFET when W is 100μm.

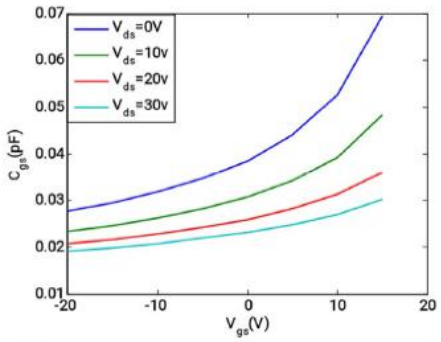


Fig. 3. The relationship between gate to source capacitance (pF) and gate to source voltage (V) in GaN MESFET.

In the light of (4), the intrinsic gate delay depends on gate to source capacitance, gate to drain capacitance, and transconductance. In particular, the mutual effect of the parasitic capacitances hinders the predictable switching behavior of careers while passing through the channel of GaN MESFET.

The gate to source voltage has been varied within a wide range incorporating both positive and negative polarities as well as zero value. By observing the characteristics curve illustrated in Fig. 4, it can be clearly understood that it is possible to reduce the intrinsic gate delay by means of applying more positive gate to source voltage and a remarkable point is that the delay almost diminishes for voltage larger than 17V

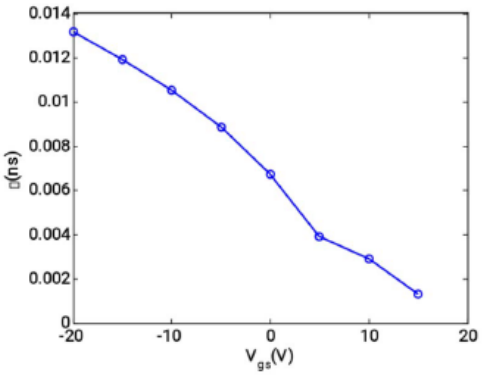


Fig. 4. The relationship between Intrinsic gate delay (ns) and gate to source voltage (V) in GaN MESFET.

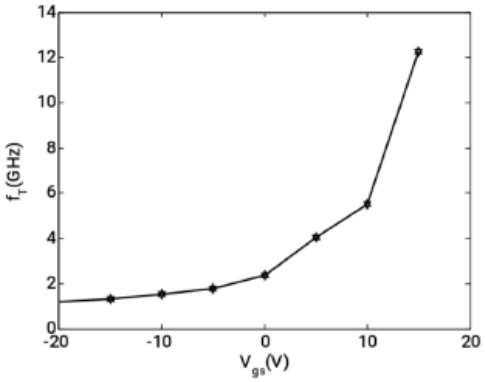


Fig. 5. The relationship between cutoff frequency (GHz) and gate to source voltage (V) in GaN MESFET.

The characteristics curve outlined in Fig. 5 can be considered as the most compelling evidence of the inverse relationship between the cutoff frequency and intrinsic gate delay. It is apparent that notwithstanding intrinsic gate delay decreases with the more positive gate to source voltages, cutoff frequency increases significantly in the range of gigahertz. the respective impacts of the variation in gate to source voltage on these properties have been investigated by analyzing the individual characteristic curves. As reported, the gate to drain capacitance drops with the rise of drain to source voltage where the characteristics curves for the greater negative value of gate to source voltage experience larger diminution. On the contrary, the gate to source capacitance rises with the increase in gate to source voltage and the slope of each characteristic curve is sharper as well due to the application of positive gate to source voltages whereas the capacitance differs more abruptly if the gate to source voltage is reduced.

## 3.3 Effect of temperature on (IV) statics characteristics of GaAs MESFET.

The static properties of GaAs MESFET has been determined from an original analytical study based on the resolution of the semiconductor fundamental equations. Then it studied the equation of thermal resistance as a function of the physical parameters of MESFETs by analogy electric thermal resistance RTH has been determined as the ratio of the difference of temperature on the thermal dissipation. The model took into account the difference between the temperature of the component and the ambient temperature and the effect of temperature on the parameters of the component.

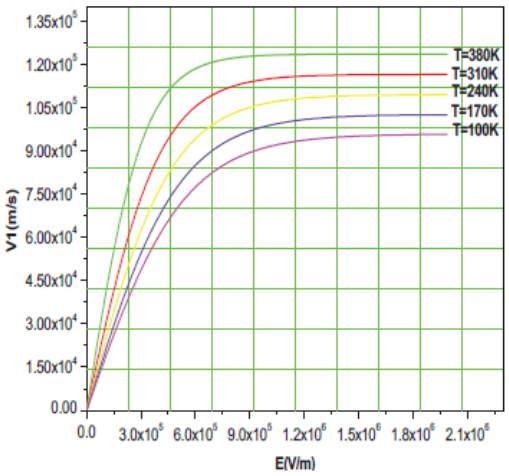


Figure 2. Variation of the velocity $V_1$ versus electric field for different values of temperatures.

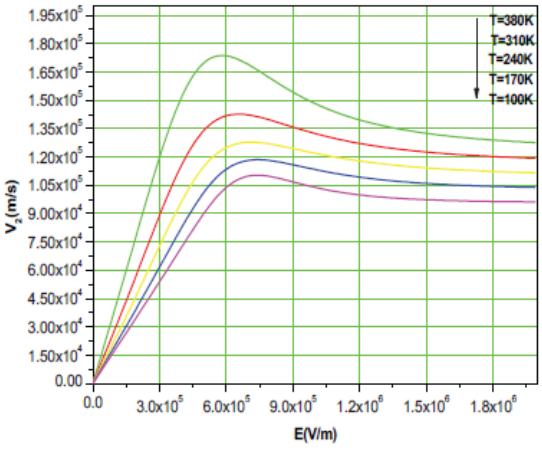


Figure 3. Variation of the $V_2$ velocity versus electric field for different values of temperatures.

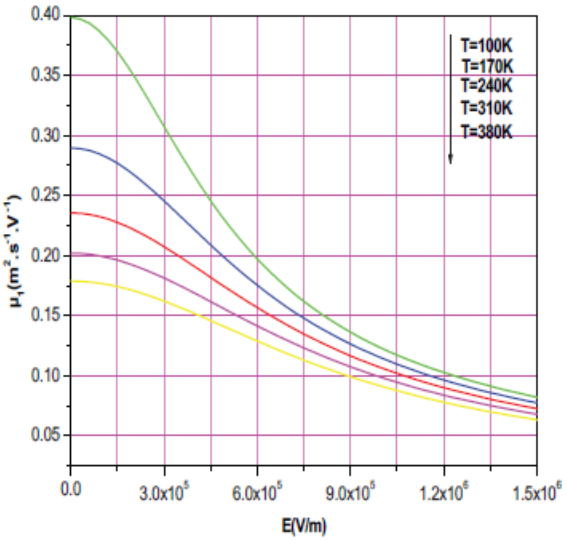


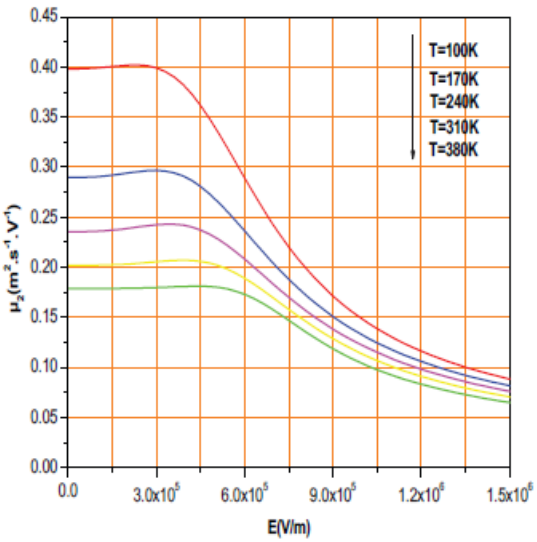


## 3.4 Analysis of Temperature Effect on MOSFET Parameter using MATLAB

This paper deals with analysis of temperature effect on some of the MOSFET parameters like bandgap, carrier mobility, saturation velocity and contact region resistance. The analysis of all the effect is done by using mathematical simulation. The overall impact of these parameters on the characteristics of the MOSFET have been analyzed A high end device should be productive efficiently and exhibits good performance for a high range of temperature. In order to optimize

the performance of the device, the parameter that comes in the case of MOSFET scenario are bandgap optimization, subthreshold leakage issue, carrier mobility and saturation velocity, the resistance at contact and interface like source and drain. This work is focused on analyzing the variation of each of these parameters with the variation in temperature. This effect of temperature on the device parameters, only if analyzed and modelled, its effect on device performance can be known and hence the better performing highly reliable device can be developed.

Carrier mobility can be considered as one of the crucial temperature dependent MOSFET parameter. The conductivity of a semiconductor is directly proportional to the product of carrier concentration and carrier mobility. Whenever all the things are equal, higher mobility leads to better device performance.

Factors depends up on the mobility of carriers in the semiconductors are donor and accepter concentration, defect concentration, and also the temperature. From the Bose-Einstein distribution, it reveals that phonon scattering is strongly a temperature dependent parameter. Since the density of phonon increases with temperature, which causes increase in scattering. [4]. Thus lattice scattering lowers the carrier mobility more and more at higher temperature. The carrier mobility is the vital parameter for the numerical simulation of the electrical characteristics on semiconductor devices. In order to capture the dependence of mobility on temperature, doping, and the electric field, different mathematical models were developed.

From the figure 2 the value of carrier velocity for Si at room temperature, 300K is 0.14 m2/V.s which matches the theoretical value [6]. A 100o C, in temperature may decrease the mobility by as much as 40%. The result is a proportional decrease in drain current, for a fixed applied voltage.so current consumption of the entire circuit may decrease considerably at high temperature. The maximum speed of operation thus decreases in proportion. The change in threshold voltage and mobility affects the drain current, the Trans conductance, and the drain to source ON resistance of MOSFET.

$$\mu(T) = \mu(T_r)(\frac{T}{T_r})^{k\mu} \quad (2)$$

Where,

T = Absolute temperature,
Tr = Room temperature
kμ = Fitting parameter with a typical value of about 1.5
$\mu(T_r)$ =ref. temp (300K) = 0.14 $m^2$/v.s

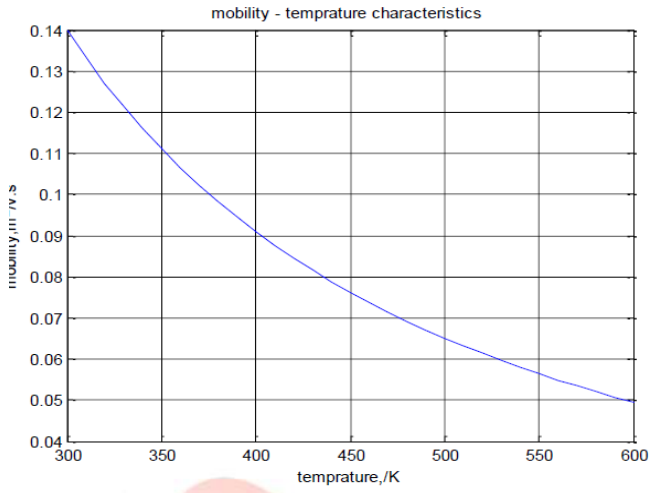


**Figure 2. The temperature dependence of the mobility.**

Evaluation of temperature dependence of the device characteristics is important for designing scaled down MOS integrated circuit that generally operates over a wide range of temperature It is well known that the change in the operating temperature of a device will influence its characteristics and hence the circuit performance. Accurate description of temperature effects in a device is necessary for a circuit level MOSFET model to predict circuit behaviors over a range of temperature. An IC does not always work under room temperature. Some effects are not prominent in room temperature, have adverse effect in higher temperature ranges.Temperature analysis done in reliability perspective can be used for performance enhancement.

## 3.5 Two-Dimensional Modeling of Nonuniformly Doped MESFET Under Illumination

A two-dimensional numerical model of an optically gated GaAs MESFET with non uniform channel doping has been developed. This is done to characterize the device as a photo detector.

First photo induced voltage (Vop) at the Schottky gate is calculated for estimating the channel profile. Then Poisson's equation for the device is solved numerically under dark and illumination condition. The paper aims at developing the MESFET 2-D model under illumination using Monte Carlo Finite Difference method. The results discuss about the optical potential developed in the device, variation of channel potential under different biasing and illumination and also about electric fields along X and Y directions. The Cgs under different illumination is also calculated. It has been observed from the results that the characteristics of the device are strongly influenced by the incident optical illumination.

**Electric field calculation**

The electric field along x and y direction have been obtained by solving following equations [9, 10]

$$E_x = \frac{\psi(i+1, j) - \psi(i-1, j)}{2mx} \quad (12)$$

$$E_y = \frac{\psi(i, j+1) - \psi(i, j-1)}{2my} \quad (13)$$

These equations have been utilized for estimating the field dependent mobility and the drain current characteristics equation.

**Mobility model**

The field dependent mobility is given by [12]

$$\mu_n(E_x) = \mu_0 + \frac{2(-2\mu_0 E_c + 3v_{sat1})}{E_c^2} E_x + \frac{3(\mu_0 E_c - 2v_{sat1})}{E_c^3} E_x^2 \quad (14)$$

where

$\mu_o$ Low field electron mobility

$V_{sat1}$ Saturation velocity

$E_c$ Critical field

The velocity-field characteristic of electrons in GaAs is assumed, i.e [13].

$$v(E) = \frac{\mu_0 E + v_s (E / E_c)^4}{1 + (E / E_c)^4} \quad (15)$$

where

$$E = \sqrt{E_x^2 + E_y^2} \quad (16)$$

Table 1. Parameters used in the simulation

| Parameter | Values |
|---|---|
| Channel length, L | 1.2 μm |
| Channel depth, a | 0.4 μm |
| Device width, Z | 25 μm |
| Absorption coefficient, α | $10^6$ /m |
| Minority carrier life time, τ | $10^{-8}$ s |
| Intrinsic carrier concentration, $n_i$ | 2.1 x $10^{12}$ /$m^3$ |
| Built-in voltage of Schottky gate, $\Phi_{bi}$ | 0.85 v |
| Incident optical power, $P_{opt}$ | 0, 0.2, 0.5 W/$m^2$ |
| Reflection coefficient at entrance, $R_m$ | 10% of $P_{opt}$ |
| Reflection coefficient at metal contact, $R_s$ | 10% of $P_{opt}$ |
| Temperature, T | 300 K |
| Straggle Parameter, σ | 0.1 x $10^{-6}$ m |
| Projected range, Rp | 0.2 x $10^{-6}$ m |
| Position of Fermi level below the conduction band, Δ | 0.02 eV |

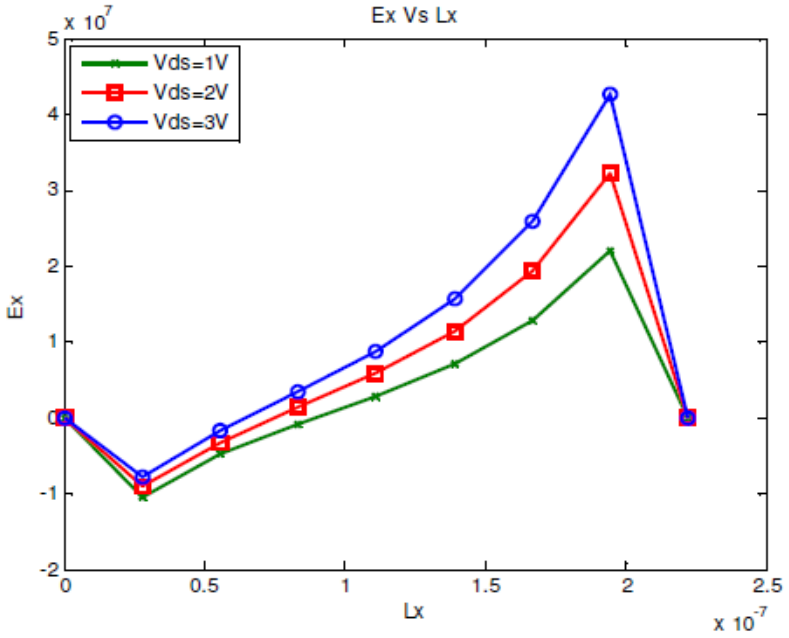


Figure 6. Ex Vs Lx for various Vds

Figure 6 shows the variation of Ex with Lx for various Vds. The plot shows that field is maximum near drain and also the plot shows that Ex increases with Vds and the effect is prominent near the drain. This is because the biasing potential is applied along X direction and at the drain

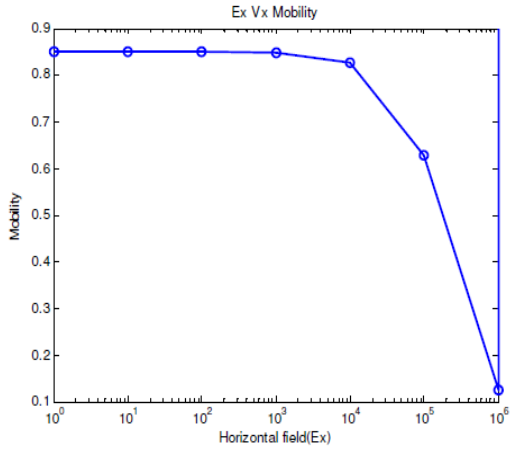


Figure 10. Mobility Vs field

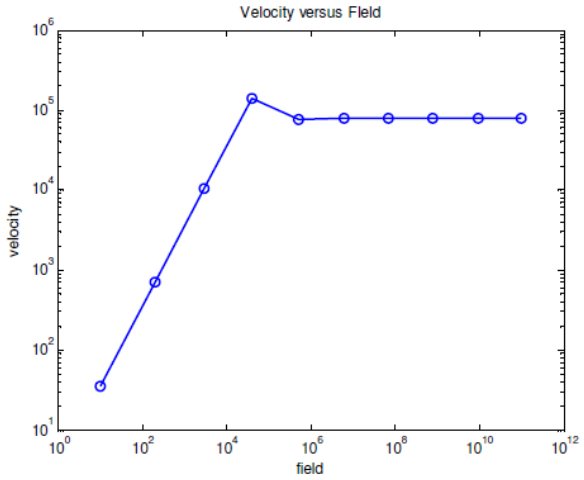


Figure 11. Carrier Velocity Vs Field

Figure 10 shows the variation in mobility along with the field and shows that the mobility is low field mobility till threshold field and decreases for higher field.

Figure 11 shows the variation of the charge velocity with the electric field. It shows that for low field the velocity of the carrier increases with the increase in the field and after threshold field the velocity reaches saturation and remains constant.

## 3.6 Quasi-Two-Dimensional Simulation of An Ion-Implanted GaAs MESFET Photodetector

A quasi-two-dimensional numerical model of an optically gated GaAs metal semiconductor field-effect transistor (MESFET) has been developed for the characterization of the device as a photodetector. The model considers the channel to be nonuniformly doped. The model involves the solution of a 1-D Poisson's equation, and takes into account the field-dependent mobility of the carriers in the channel for computation of the current. It has been found that, in a short-channel MESFET photodetector, the drain current saturation is caused by the velocity saturation of the carriers rather than pinch off. The photocurrent gain, responsivity, and the input RC time constant of an ion-implanted GaAs MESFET having a semitransparent metal gate have been estimated numerically on the basis of the model.

# Chapter 4: Modelling of MESFET DC Characteristics in different Temperature using Finite Element Analysis Software

MESFET is widely used in front end amplifier because of its excellent characteristics towards noise in high frequency application. To establish its supercity in high frequency application device AC equivalent circuit parameter are used. This parameter is controlled by the device manufacturing and design process. This can be examined from its electrical response.

## 4.1 Variation of drain current over drain voltage in different temperature

To analyze the GaAs MESFET (n-doped) response in different drain-source voltage, different gate voltage and for different temperature one 2D MESFET model developed in COMSOL Multiphysics. In this model MESFET biasing in different temperature (100, 170, 240, 293, 310, 380) with different gate (0V, 1V, 2V) and drain ( 0 to 10 V) voltages has been considered.

**Geometry:**

Parameter used in the model are given below

**Table 4-1 Physical parameter used in this COMSOL Model**

| Parameter Name | Parameter Value | Description |
|---|---|---|
| L | 1E-6 m | Gate length |
| Wd | 4E-6 m | Device width |
| Hd | 5E-7 m | Device height |
| Ws | 1E-6 m | Source width |
| Wdd | 1E-6 m | Drain width |
| Nd | 1E22 1/m³ | Doping |

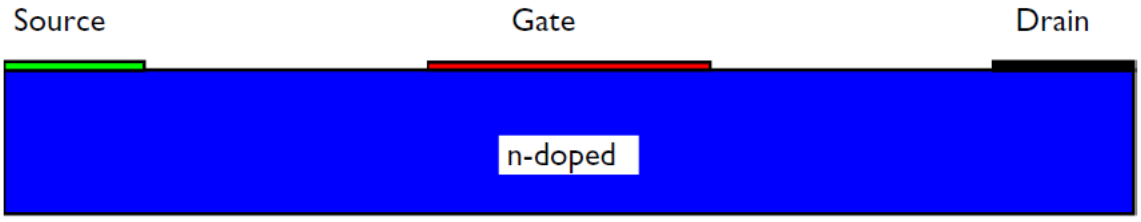


**Figure 4-1 MESFET model geometry**

**Material:**

Inbuilt GaAs material used in this model. The details of material property is given below

**Table 4-2 Material property of GaAs used in model**

| Property | variable | Value | Unit |
|---|---|---|---|
| Relative permittivity | epsilonr_iso ; epsilonrii = epsilonr_iso, epsilonrij = 0 | 12.9 | 1 |
| Band gap | Eg0 | 1.424[V] | V |
| Electron affinity | chi0 | 4.07[V] | V |
| Effective density of states, valence band | Nv | (T/1[K])^(3/2)*1.83e15[1/cm^3] | $1/m^3$ |
| Effective density of states, conduction band | Nc | (8.63e13*(T/1[K])^(3/2)*(1-1.93e-4*(T/1[K])-4.19e-8*(T/1[K])^2+21*exp(-0.29[V]*e_const/(k_B_const*T))+44*exp(-0.48[V]*e_const/(k_B_const*T))))[1/cm^3] | $1/m^3$ |
| Electron mobility | mun | 8500[cm^2/(V*s)] | $m^2/(V \cdot s)$ |
| Hole mobility | mup | 400[cm^2/(V*s)] | $m^2/(V \cdot s)$ |

**MESH:**

To study the model with better accuracy finer MESH from predefined list was chosen.

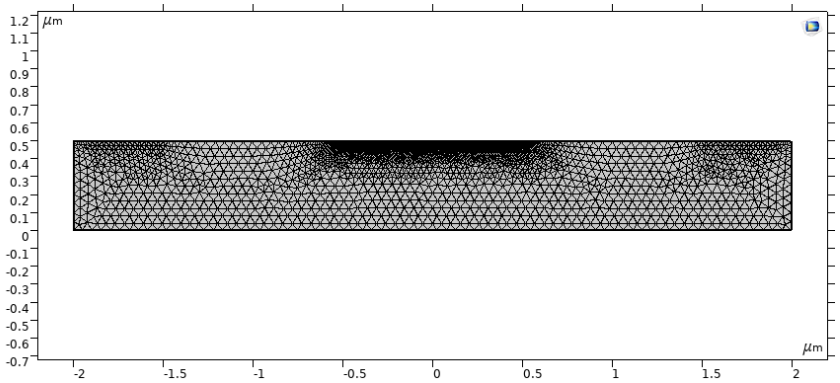

Study

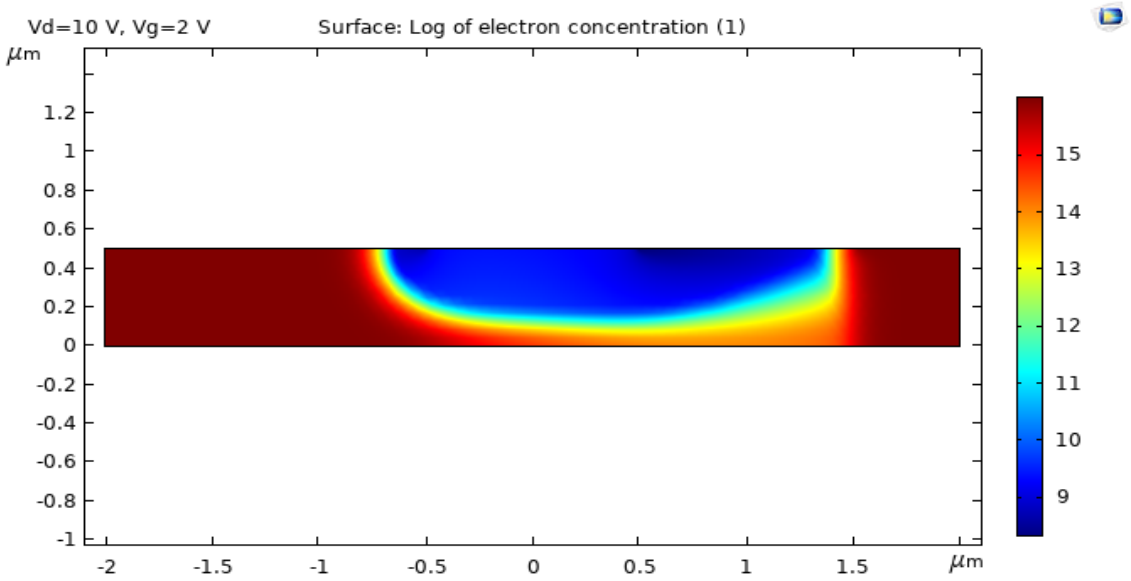


**Figure 4-2 Majority carrier concentration in different region**

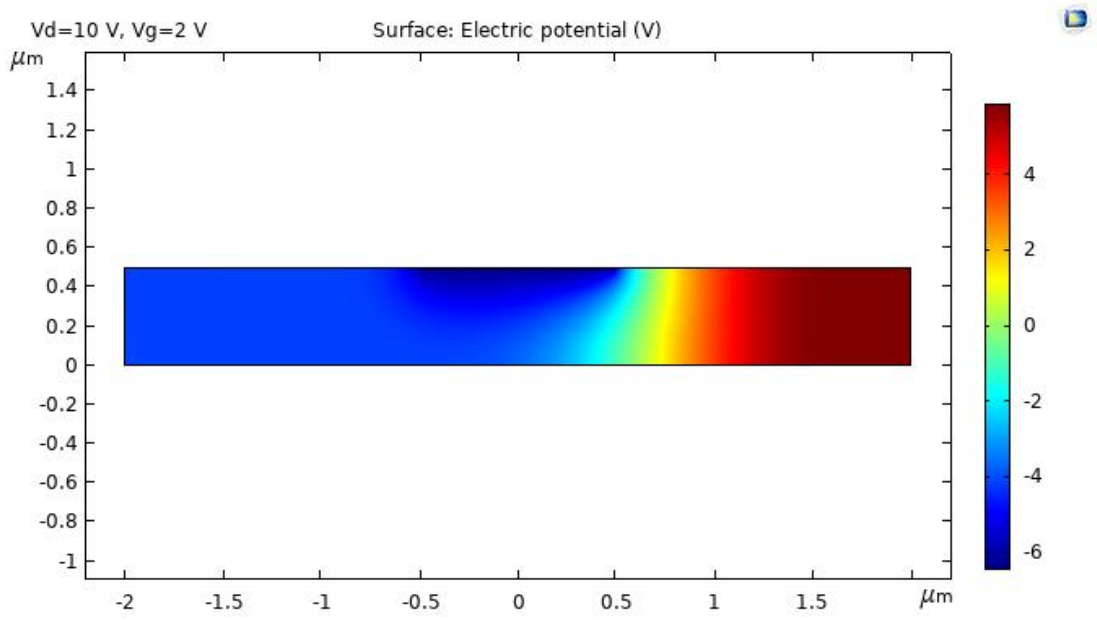


**Figure 4-3 Surface Electric potential in different region of MESFET**

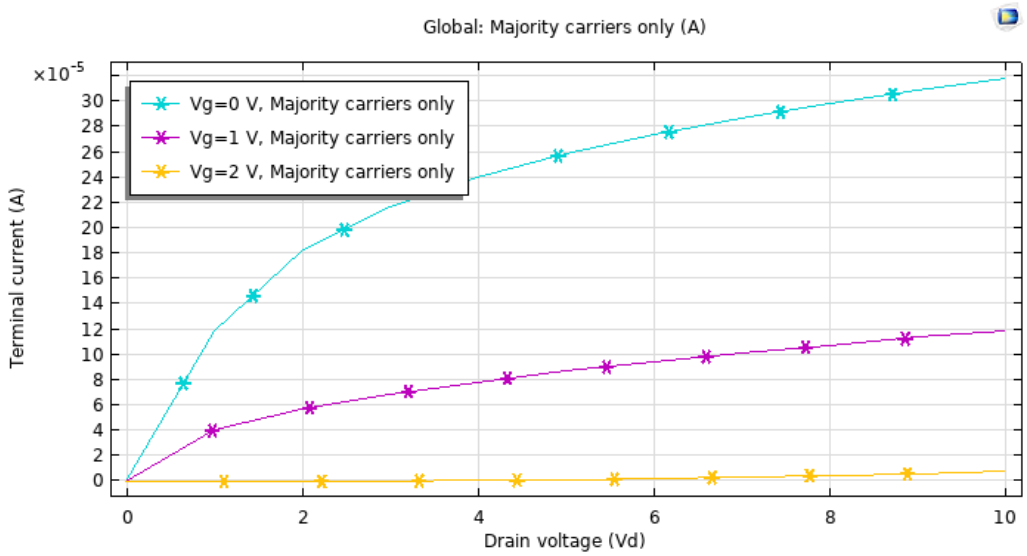


**Figure 4-4 Variation of Terminal Current with drain voltage at different gate voltage at T= 300 K**

The model was computed with different gate (0V, 1V, 2V) in drain voltages from 0 to 10 V. The above simulation was carried out in different temperature (100, 170, 240, 293, 310, 380K). The variation of terminal current $I_d$ in different values of $V_d$ (from 0 to 10 V) and at different temperature are tabled below. Here the value of $v_g = 0\,V$.

**Table 4-3 value of Id in different Temperature at Vg=0**

| Vd | Id * E-4 (T=100K, Vg=0) | Id* E-4 (T=170K, Vg=0) | Id* E-4 (T=240K, Vg=0) | Id* E-4 (T=293K, Vg=0) | Id* E-4 (T=310K, Vg=0) | Id* E-4 (T=380K, Vg=0) |
|---|---|---|---|---|---|---|
| 0 | 0 | 0 | 0 | 0 | 0 | 0 |
| 1 | 1.114015849 | 1.140068374 | 1.168583252 | 1.191365085 | 1.198776217 | 1.231467362 |
| 2 | 1.684301656 | 1.727795948 | 1.777006784 | 1.816872028 | 1.82990025 | 1.887064409 |
| 3 | 2.005176845 | 2.057238646 | 2.117075397 | 2.166005152 | 2.182060172 | 2.252665377 |
| 4 | 2.226611294 | 2.283563406 | 2.349329184 | 2.403297319 | 2.421034486 | 2.499122033 |
| 5 | 2.399338362 | 2.459589652 | 2.529272957 | 2.586538024 | 2.605371469 | 2.688316509 |
| 6 | 2.543215307 | 2.605917203 | 2.678468699 | 2.738129643 | 2.757757165 | 2.844208821 |
| 7 | 2.6677412 | 2.732381657 | 2.807179478 | 2.8687066 | 2.888951094 | 2.978119537 |
| 8 | 2.778119565 | 2.8443845 | 2.921043336 | 2.984106007 | 3.004856617 | 3.096245942 |
| 9 | 2.877538797 | 2.945258286 | 3.023547402 | 3.087938544 | 3.109124695 | 3.202414468 |
| 10 | 2.968645755 | 3.037628874 | 3.117341674 | 3.182892607 | 3.204458634 | 3.299403118 |

**Table 4-4 value of Id in different Temperature at Vg=1**

| Vd | Id * E-5 (T=100K, Vg=1) | Id* E-5 (T=170K, Vg=1) | Id* E-5 (T=240K, Vg=1) | Id* E-5 (T=293K, Vg=1) | Id* E-5 (T=310K, Vg=1) | Id* E-5 (T=380K, Vg=1) |
|---|---|---|---|---|---|---|
| 0 | 0 | 0 | 0 | 0 | 0 | 0 |
| 1 | 3.318226594 | 3.574452646 | 3.863125854 | 4.097953274 | 4.175050693 | 4.520600293 |
| 2 | 4.704548076 | 5.032749539 | 5.410272836 | 5.721286693 | 5.824021366 | 6.285327303 |
| 3 | 5.743044 | 6.110902993 | 6.536296597 | 6.887614716 | 7.003766901 | 7.524800636 |
| 4 | 6.617036458 | 7.012941867 | 7.471964916 | 7.851382546 | 7.976842487 | 8.539000888 |
| 5 | 7.387702727 | 7.805513274 | 8.29066995 | 8.691831087 | 8.824472999 | 9.418223567 |
| 6 | 8.084900375 | 8.520754165 | 9.027354866 | 9.446311911 | 9.584821811 | 10.20430993 |
| 7 | 8.725989125 | 9.177236235 | 9.702053779 | 10.13609979 | 10.27957912 | 10.92081769 |
| 8 | 9.322229686 | 9.786849134 | 10.32750554 | 10.77466804 | 10.92246481 | 11.58257321 |
| 9 | 9.880971658 | 10.35766171 | 10.91248582 | 11.37134004 | 11.52297969 | 12.19985059 |
| 10 | 10.4091367 | 10.89687163 | 11.46457808 | 11.9340392 | 12.08916129 | 12.78119697 |

**Table 4-5 value of Id in different Temperature at Vg=2**

| Vd | Id*E-6 (T=100K, Vg=2) | Id*E-6 (T=170K, Vg=2) | Id*E-6 (T=240K, Vg=2) | Id*E-6 (T=293K, Vg=2) | Id*E-6 (T=310K, Vg=2) | Id*E-6 (T=380K, Vg=2) |
|---|---|---|---|---|---|---|
| 0 | 0 | 0 | 0 | 0 | 0 | 0 |
| 1 | 6.47E-10 | 2.52974E-06 | 0.000555185 | 0.007863968 | 0.016316658 | 0.238106467 |
| 2 | 1.6003E-08 | 0.000167718 | 0.00943683 | 0.05931616 | 0.095129692 | 0.545273861 |
| 3 | 3.01169E-06 | 0.003274197 | 0.067177123 | 0.256000816 | 0.35734933 | 1.179980032 |
| 4 | 0.000170068 | 0.029748215 | 0.266500826 | 0.702688893 | 0.896131396 | 2.141992675 |
| 5 | 0.004016874 | 0.149515712 | 0.700412743 | 1.431219891 | 1.720558003 | 3.367893865 |
| 6 | 0.044196396 | 0.466301127 | 1.394495003 | 2.408787874 | 2.785658903 | 4.788516406 |
| 7 | 0.23113795 | 1.031941539 | 2.317641355 | 3.582472964 | 4.035843074 | 6.348139058 |
| 8 | 0.671128858 | 1.827674403 | 3.422429504 | 4.903904751 | 5.423709013 | 8.006087522 |
| 9 | 1.360499462 | 2.808049823 | 4.665385043 | 6.334911364 | 6.912884625 | 9.733545941 |
| 10 | 2.248958765 | 3.933335832 | 6.016512766 | 7.851540417 | 8.48114875 | 11.51488814 |

The above data has been plotted and we have the following graph.

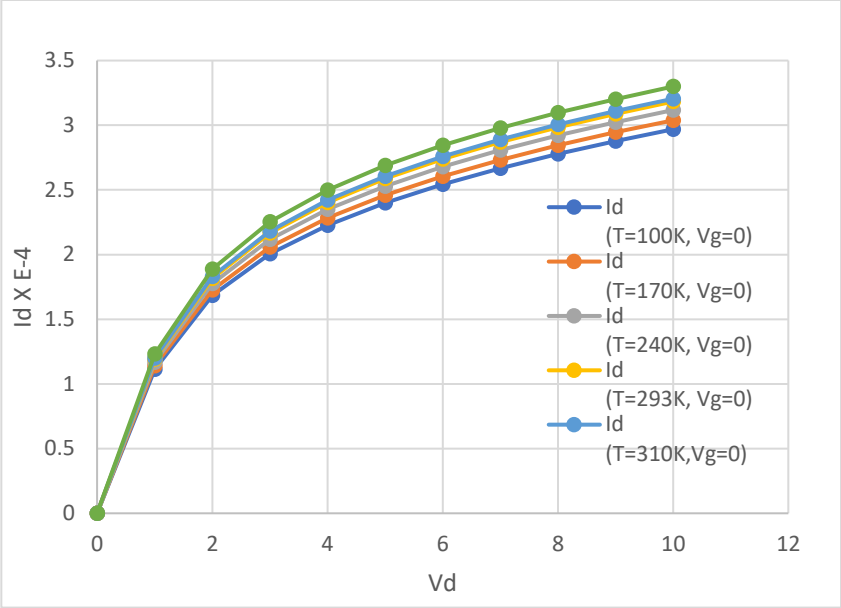


**Figure 4-5 Id vs Vd at Vg = 0 in different temperature**

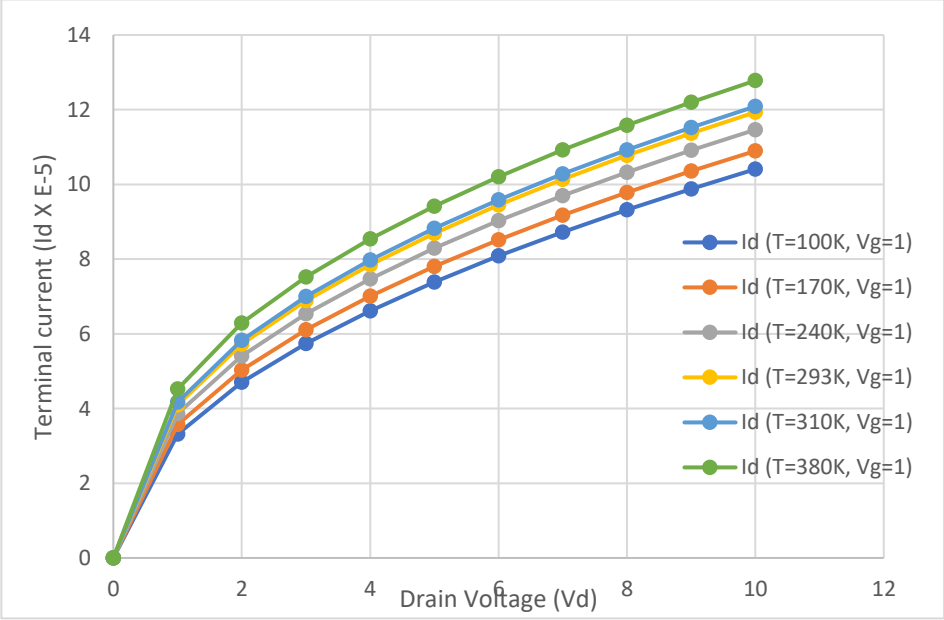


**Figure 4-6 Id vs Vd in different temperature at Vg=1 V**

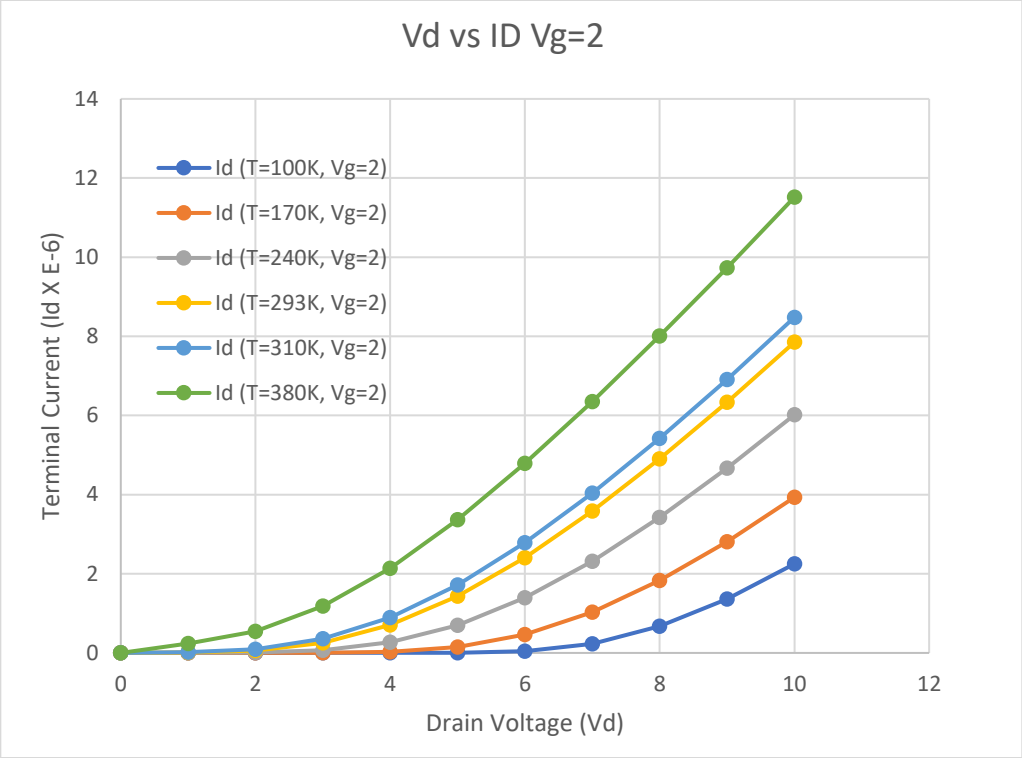


**Figure 4-7 Id vs Vd in different temperature at Vg=2 V**

# Chapter 5: Effect of Applied Electric Field and Temperature on Mobility and Carrier velocity.

The dependence of electron drift velocity on the applied field remains one of the most important relations require in the numerical simulation of GaAs devices

For low electric field the carrier mobility remains constant and varies from one material to another, and the carrier velocity is directly proportional to the electric field. It is defined by the equation [5].

$$V(E) = \mu_0 E \dots\dots\dots\dots (6.1)$$

$\mu_0$: the mobility of electrons at low electric field.

However, when the applied electric field becomes important, the electron transfer intervals induced in the GaAs a decrease of the carrier velocity and leads to strong negative differential mobility [6].

This decrease results in a non-linear variation of the drift velocity of the carriers. Therefore, several approximate analytical expressions have been proposed for this function [7].

For our study, we have tested two mobility laws for the reason that they have good approximations comparing to the experimental data. When E<E0 which corresponds to the critical field, the two expressions are given by:[1]

First expression [8], [9]:

$$\mu_1 = \frac{\mu(T) + V_s\left(\frac{E^3}{E_c^4}\right)}{1 + \left(\frac{E}{E_c}\right)^4} \dots\dots\dots\dots\dots\dots (6.2)$$

$$v_1 = \mu_1 E = \frac{\mu(T) + V_s\left(\frac{E^3}{E_c^4}\right)}{1 + \left(\frac{E}{E_c}\right)^4} . E \dots\dots\dots\dots\dots\dots (6.2a)$$

Second expression [10]

$$\mu_2(E) = \frac{v_s}{E}\tanh\left(\frac{\mu(T)E}{v_s}\right) \dots\dots\dots\dots\dots (6.3)$$

$$E_c = \frac{v_s}{\mu(T)} \quad [11]$$

$$E_0 = \frac{1}{2}\left[ E_s + ( E_s^2 - 4E_c^2)^{\frac{1}{2}}\right]$$

$$v_2 = \mu_2 . E = v_s \tanh\left(\frac{\mu(T)E}{v_s}\right) \dots\dots\dots\dots\dots (6.3a)$$

Another expression for the velocity is given by:[1]

$$v_n(E) = \mu_n(E)E = \frac{\mu(T)E}{1 + \left(\frac{E}{E_c}\right)^2} \dots\dots\dots\dots\dots\dots (6.4)$$

So, the expression of mobility is as follows:

$$\mu_n(E) = \frac{\mu(T)}{1 + \left(\frac{E}{E_c}\right)^2} \dots\dots\dots\dots\dots\dots\dots\dots (6.5)$$

The dependence of carrier mobility with temperature

$$\mu(T) = \mu_0(T_R)\left[\frac{T}{T_R}\right]^{0.6} \dots\dots\dots\dots (6.6)$$

$$\mu_0(T_R) = 3740\ cm^2 S^{-1} V^{-1}$$

$$T_R = Room\ Temperature$$

Final expression of mobility:

$$\mu_1 = \frac{3740\left[\frac{T}{300}\right]^{0.6} + V_s\left(\frac{E^3}{E_c^4}\right)}{1 + \left(\frac{E}{E_c}\right)^4} \dots\dots\dots\dots\dots\dots (6.7)$$

$$\mu_2(E) = \frac{E_c 3740\left[\frac{T}{300}\right]^{0.6}}{E} \tanh\left(\frac{E}{E_C}\right) \dots\dots\dots\dots\dots (6.8)$$

$$\mu_n(E) = \frac{3740\left[\frac{T}{300}\right]^{0.6}}{1 + \left(\frac{E}{E_c}\right)^2} \dots\dots\dots\dots\dots\dots\dots\dots (6.9)$$

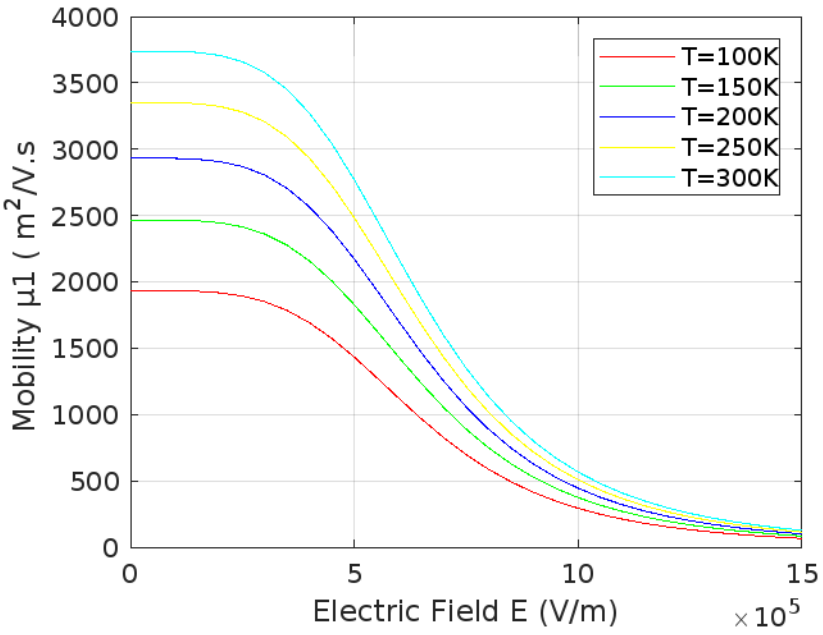


**Figure 5-1Variation of $\mu_1$ mobility with electric field for different values of temperature**

Matlab code of the above plot is given in Chapter 9.

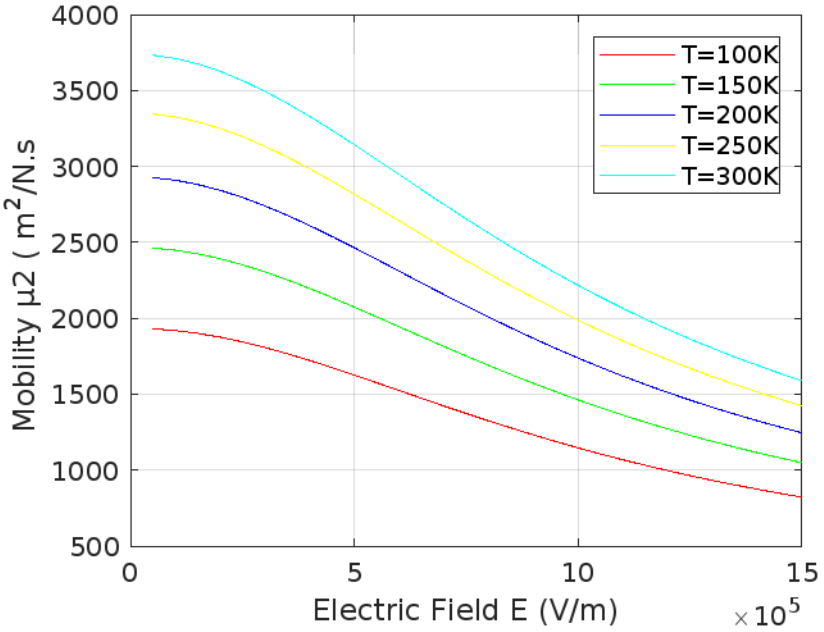


**Figure 5-2 1Variation of $\mu_2$ mobility with electric field for different values of temperature**

Matlab code of the above plot is given in Chapter 9.

The curve us linear as compared to $\mu_1$mobility.

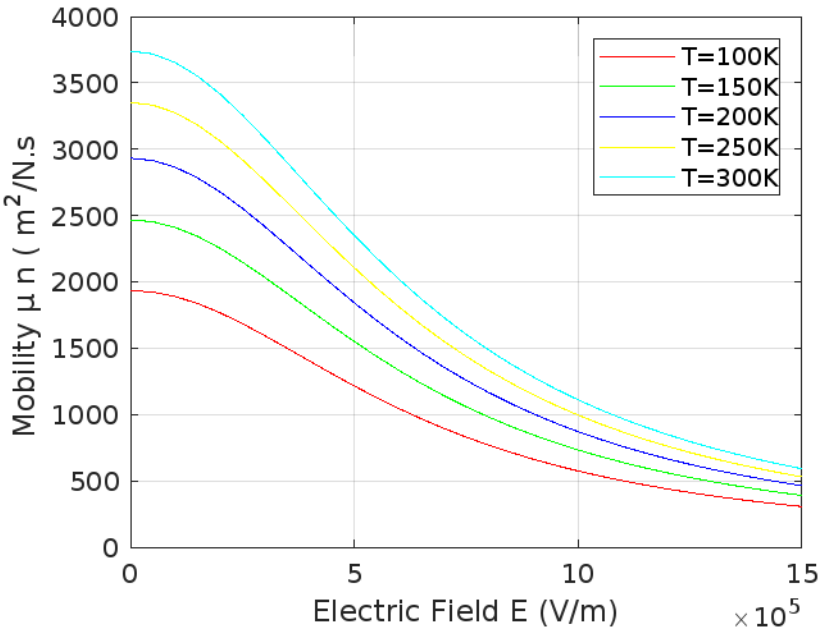


**Figure 5-3 Variation of $\mu_n$ mobility with electric field for different values of temperature**

Matlab code of the above plot is given in Chapter 9.

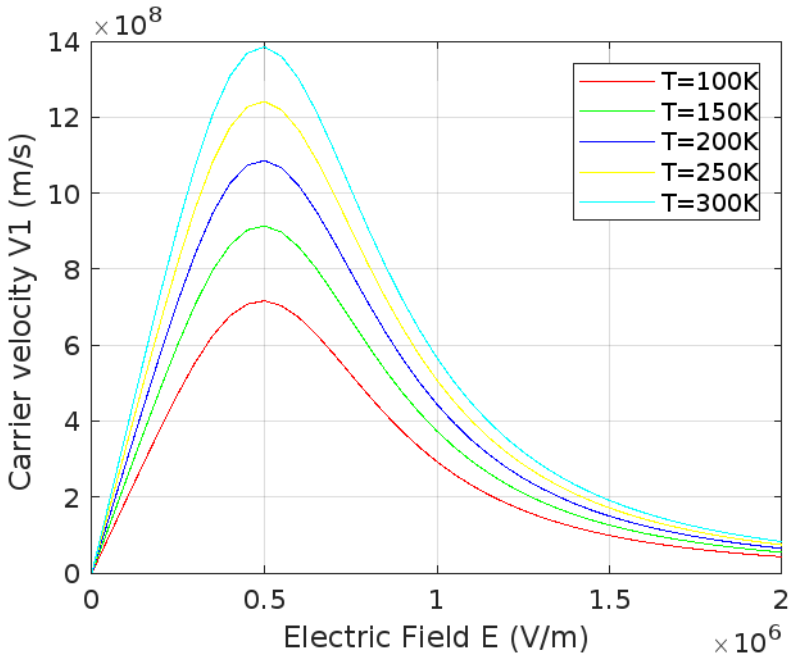


**Figure 5-4 representation of carrier velocity v1 as a function of applied electric field in different temperature**

Matlab code of the above plot is given in Chapter 9.

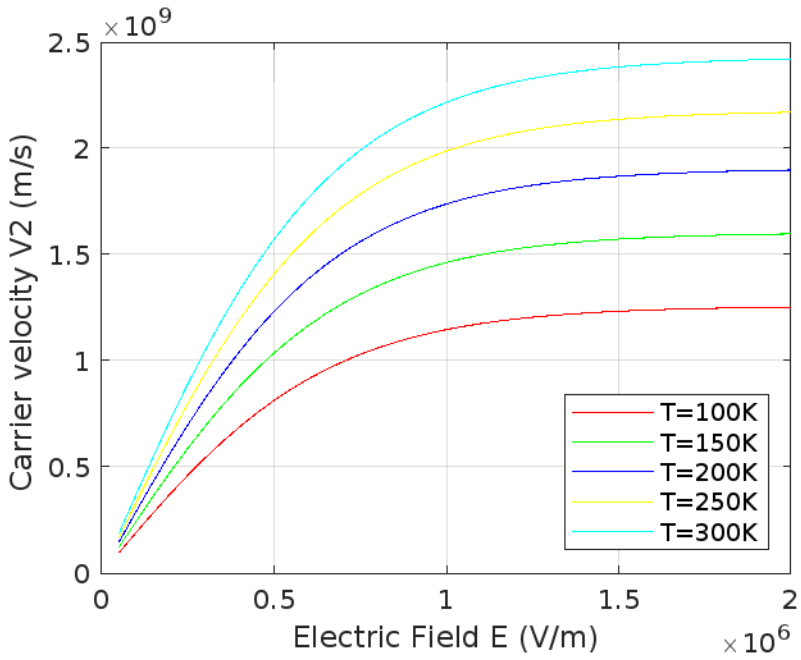


**Figure 5-5 representation of carrier velocity v2 as a function of applied electric field in different temperature**

Matlab code of the above plot is given in Chapter 9.

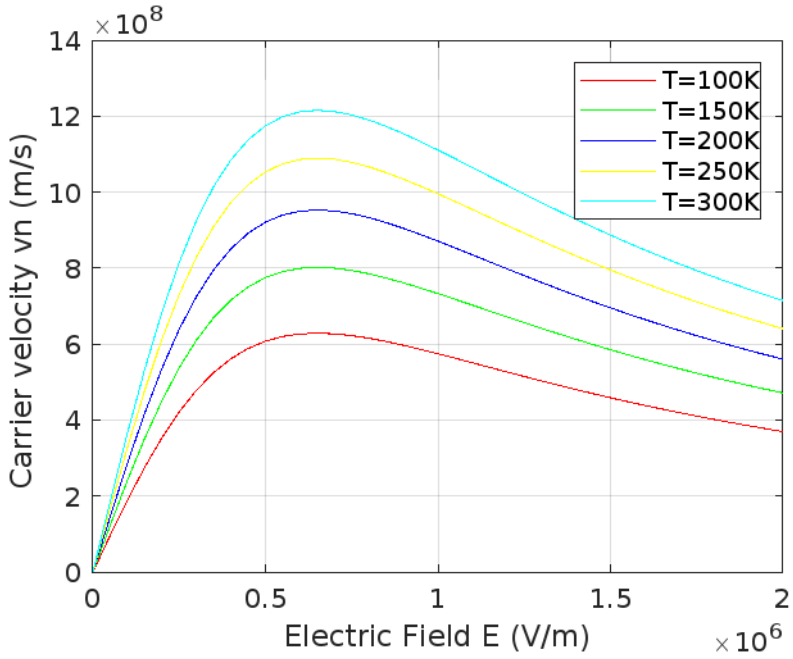


**Figure 5-6 representation of carrier velocity vn as a function of applied electric field in different temperature**

Matlab code of the above plot is given in Chapter 9.

$$L = 4\ \mu m$$

$$a = 0.3\ \mu m$$
$$Z = 360\ \mu m$$
$$N_d = 6.7e16\ cm^{-3}$$
$$\mu_0 = 3740\ cm^2\ S^{-1}V^{-1}$$
$$B_{bi} = 0.8\ V$$
$$R_s = 16\ \Omega$$
$$R_D = 16\ \Omega$$

The figure 5-1, figure 5-2, figure 5-3 shows that the mobility is higher as the temperature decreases. Five values of temperature T=100,150,200,250,300 K has been chosen. From thsese figure it is found that performance and reliability of the transistor are strongly influenced by the temperature. Conduction along with the channel is due to the majority carrier (electrons), it will be affected by the temperature variation for certain parameters (electron mobility, the Schottky barrier height, the saturation velocity, the dielectric constant and the same the specific resistance of ohmic contacts). If the temperature increases, thermal motion of the carriers also increases and hence the electron mobility of the channel. decreases from expression , which causes a decrease in the current "Ids". Similarly, the height of the potential barrier increases with increasing temperature from expression (8), therefore the width of the space charge region increases against the conductive channel narrows, and thus the drain current decreases.

# Chapter 6: Numerical Calculation of Parameters

## 6.1 Calculation of the Electric field, potential and the drain current in the Channel.

To calculate the potential and the electric field under the gate, the channel is divided into two principal regions as shown in Figure 5.1 [1]

a. The first region (1) the gate directly is controlled by the gate.[1]

b. The second region (2) outwards of the first region known as region not controlled by the gate.[1]

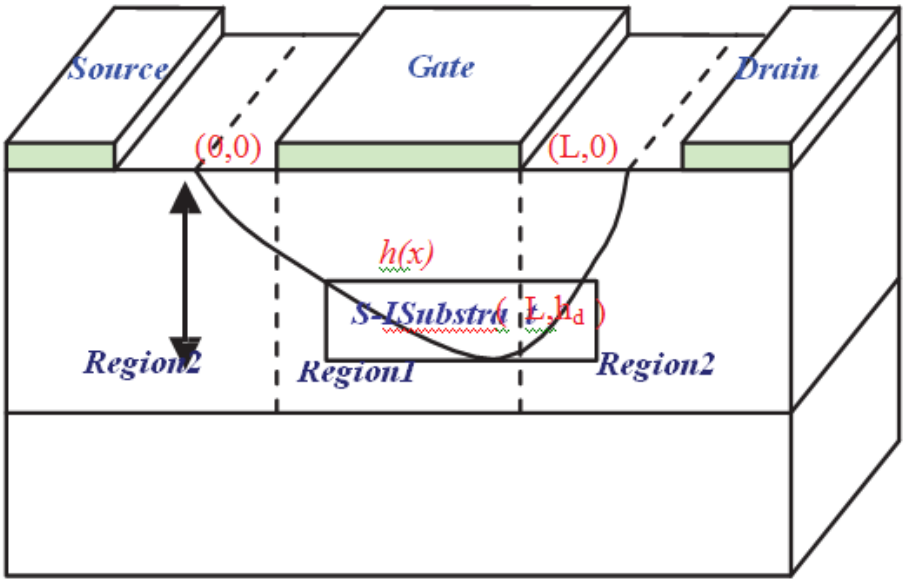


**Figure 6-1 Depletion Regions: (1) Controlled by the gate, (2) Not Controlled by the gate**

The electric potential due to the electrical charge formed under the gate can given by [2]:

$$V_q(x,y) = \int_0^y \frac{eN_d(x,y)}{\varepsilon} y dy + y\int_y^{h(x)} \frac{eN_d(x,y)}{\varepsilon} dy + Vb_i - V_g \dots\dots\dots\dots\dots\dots\dots (1)$$

$N_d(x,y) = N_d(y) - n(x,y)$,

Where $N_d(y)$ is the density of the donors that varies with y direction. and $n(x,y)$ is the free electrons density in the depletion layer. $V_{bi}$ is the built-in Schottky barrier gate potential and ε is the abbreviation of permittivity.

It should be noted that the approximations in (1) is based on the fact that the depletion layer thickness under the gate $h(x)$ is a slowly varying function in the channel and is giving by:

$$h(x) = \left[\frac{2\varepsilon(V_{bi} - V)}{qN_d}\right]^{1/2} \dots\dots\dots\dots\dots\dots\dots\dots\dots (2)$$

The channel potential is obtained by integration limit with $y = h(x)$

$$V(y) = \frac{qn_d}{\varepsilon}\left[hy - \frac{Y^2}{2}\right] \dots\dots\dots\dots\dots\dots\dots\dots\dots (3)$$

The equation of the potential takes a maximum of values in diffusion potential $V_{bi}(y = h)$.

$$V_b = V(y = h) - V(y = 0) \dots\dots\dots\dots\dots\dots\dots\dots (4)$$

The dimensional potential of the channel under the gate is given as follows:

$$V(x) = \frac{qN_d h^2(x)}{2\varepsilon} + V_g - V_{bi} \dots\dots\dots\dots\dots\dots\dots\dots (5)$$

Calculation of drain current in the channel:

Some approximation needs to make to calculate drain current equation as a function of drain voltage. [3]

a. Neglects the current flow in the y-direction. This approximation is valid for the components with the short length gate.

b. An abrupt junction Schottky barrier.

c. A channel dopped uniformly $N_d(x,y) = N_d$, $N_d$ is constant.

d. Neglect the edge effects,

The Current density expression given as:

$$J_x = \sigma(x,y,z).E_x \dots\dots\dots\dots\dots\dots\dots\dots\dots (6)$$

With $\sigma(x,y) = \rho(y)\mu_n.(E_x)$

$$J_x = qN_d\mu_n E_x = -q\mu_n N_d \frac{dV(x)}{dx} \dots\dots\dots\dots\dots\dots\dots (7)$$

$\mu_n(E_x)$ is the electric field which depends on the electric field.

The drain current Id is obtained by integrating the $J_x$ across conductor section of the channel:

$$I_d = -\int_0^Z \int_{h(x)}^a J_x dydz = -Z\int_{h(x)}^a J_x dy \dots\dots\dots\dots\dots\dots\dots\dots\dots\dots\dots (8)$$

$$V_x(E_x) = \mu_n E_x(x)$$

The above calculation does not consider the contribution depletion layer, we put:

$I_p = (qN_d)^2\mu_n Z a^3$

$q$: $electron\ charge.$

$N_d$: $carrier\ density\ in\ the\ chanel$

$a$: $chanel\ thicknes$

$L$: $mIntrinsic\ chanel\ length\ (controlled\ by\ the\ gate)$

$$V_p = q\frac{N_d a^2}{2\varepsilon} = V_{bi} - V_g$$

$$a = \left[\frac{2\varepsilon}{qN_d}\left(V_{bi} - V_g\right)\right]^{\frac{1}{2}}$$

$$\frac{h(x)}{a} = \left[\frac{V_{bi} + V(x) - V_g}{V_{bi} - V_g}\right]$$

$The\ final\ expression\ of\ the\ current\ I_d[4] is\ given\ by$

$$I_d(V_d, V_g) = I_p\left[\frac{V_d}{V_p} - \frac{2}{3}\left[\left(\frac{V_d + V_{bi} - V_g}{V_p}\right)^{\frac{3}{2}} - \left(\frac{V_{bi} - V_g}{V_p}\right)^{\frac{3}{2}}\right]\right] \dots\dots\dots\dots\dots\dots\dots\dots\dots\dots (9)$$

The general expression of Drain-Source current in the linear region is given below. This includes parasitic source and drain resistance.

$$I_{ds} = \frac{qZ\mu N_d a}{L}\left(V_{ds} - I_{ds}(R_s + R_d) - \frac{2}{3V_p^{\frac{1}{2}}}\left[\left(V_{bi} - V_{gs} + V_{ds} - I_{ds}R_d\right)^{\frac{3}{2}} - \left(V_{bi} - V_{gs} + I_{ds}R_s\right)^{\frac{3}{2}}\right]\right)$$

…… (10)

Where

$I_{ds}$ : $current\ from\ \ drain\ to\ source$

$\mu$ : $mobility\ of\ electron$

$A$ : $thickness\ of\ active\ channel$

$Z$ : $gate\ width$

$L$ : $gate\ length$

$V_{ds}$ : $drain - source\ voltage$

$R_s$ : $parasitic\ source$

$R_d$ : $drain\ resistances$

$V_p$ : $pinch - off\ voltage$

To get the value of current multiple iteration has been done to solve the equation . Velocity saturation occurs when electric field in the channel start increases.

The Length of the channel ( $L_s$)$is\ given\ by$:

$$L_s = L - \frac{2a}{\pi}\sin^{-1}\left(\frac{\pi K_d(V_{ds} - V_{1s})}{2aE_s}\right) \ldots\ldots\ldots\ldots\ldots\ldots\ldots\ldots\ldots\ldots (11)$$

The Gate length spacing $L'_s$ is given by

$$L'_s = \frac{(1 - K_d)V_{2s}}{E_s \cosh\left(\frac{\pi L_s}{2a}\right)}$$

Where

$K_d$ = voltage drop ratio in the region of high field to that in the conducting channel.

$V_{(2)S}$ = voltage drops in the channel.

Drain-current ($I_{dsat}$) in the saturation region

$$I_{dsat} = \frac{1 + 2\beta R_s(V_{gs} - V_t) - \left(1 + 4\beta R_s(V_{gs} - V_t)\right)^{\frac{1}{2}}}{2\beta R_s^2} \ldots\ldots\ldots\ldots\ldots\ldots\ldots (12)$$

Where

$$\beta = \frac{2\varepsilon_s V_{sat} Z}{a(V_p + 3E_s L_s)}$$

$$V_t = V_{bi} - V_p$$

For $V_{ds} > V_{sat}$ the drain current $I'_{dst}$ become

$$I'_{dsat} = I_{dsat}\left(1 + \frac{L_s + L'_s}{L}\right) \ldots\ldots\ldots\ldots\ldots\ldots\ldots\ldots\ldots\ldots (13)$$

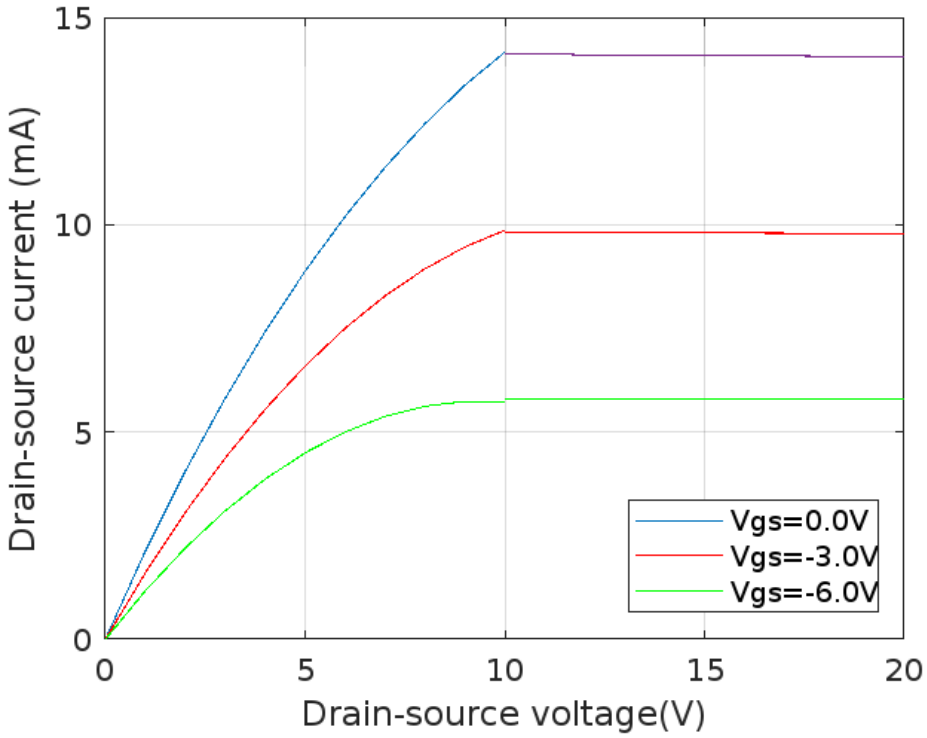


**Figure 6-2 Ids-Vds characteristics for GaN MESFET**

MATLAB Code used to obtain the figure 5.2 is given in Chapter-9 MATLAB Code

**Table 6-1 Characteristics of MESFET used in Matlab Simulation**

| | $L$ $(\mu m)$ | $A$ $(\mu m)$ | $Z$ $(\mu m)$ | $N_d$ $(cm^{-3})$ | $\mu_n$ $(cm^2S^{-1}V^{-1})$ | $V_{bi}$ $(V)$ | $R_s$ $(\Omega)$ | $R_D$ $(\Omega)$ |
|---|---|---|---|---|---|---|---|---|
| MESFET | 4 | .3 | 360 | 6.7e16 | 3740 | 0.8 | 16 | 16 |

Figure 5-2 shows the variation of the drain-to-source current with the drain-to-source voltage for a fixed applied gate voltage *Vg = (0,-3.0, -6.0)* V. The velocity saturation of the carriers occurs much earlier before the depletion regions gate and substrate. touch each other to cause the pinch off.

## 6.2 Transconductance

Transconductance plays an important role in determining the quality of MESFET specially for designing high frequency application. It can be calculated by taking the derivative of channel current $(I_{ds})$ with respect to gate -source voltage $(V_{gs})$ keeping drain to source voltage $(V_{ds})$ constant.

$$g'_m = \frac{g_m}{1 + G_m R_s} \ldots\ldots\ldots\ldots\ldots\ldots (5..2.1)$$

where,

$$g_m = \frac{\partial I_{ds}}{\partial V_{gs}} \ where\ V_{ds} is\ constant \ldots\ldots\ldots\ldots\ldots\ldots (5.2.2)$$

$$g' is\ the\ effective\ transconductance$$

Final expression of the transconductance is given as [3]

$$g_m = q\mu N_D W t_e \left[ \left( V_{ga} + V_{bi} - V_{gs} \right)^{\frac{1}{2}} - \frac{\left( V_{bi} - V_{gs} \right)^{\frac{1}{2}}}{V_p^{\frac{1}{2}}} \right] \ldots\ldots\ldots\ldots\ldots (5.2.3)$$

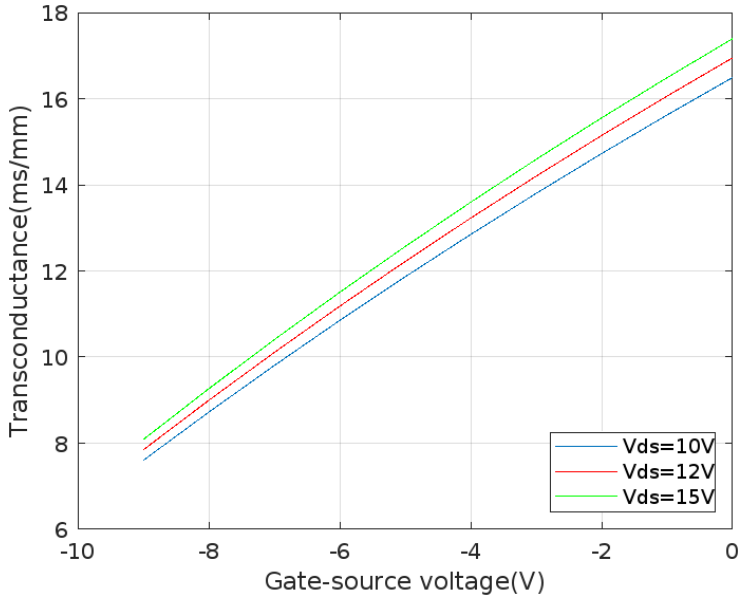


**Figure 6-3 Transconductance as a function of gate source voltage for different Vds**

MATLAB code used to obtain this plot is given in Chapter-9 MATLAB Code

Where,

$N_d = 1x10^{18}cm^{-3}$, channel doping concentration

$N_a = 1x10^{15}cm^{-3}$, substrate doping

$L = 1x10^{-4}cm$, gate- length

$Z = 100x10^{-4}cm$, device width

a $= 0.3x10^{-4}cm$. active channel thickness

From the figure 5.4.it is seen that transconductance decrease with the increase of negative gate voltage as the depletion layer increased and channel layer width decreases. Which results drain current to decreases.

## 6.3 Drain Conductance:

The drain conductance is obtained by differentiating Chanel current with $V_{ds}$ keeping gate to source voltage constant ($V_{gs}$) . The expression of drain conductance is written as

$g_d = \frac{\partial I_d}{\partial V_{ds}}\ where\ V_{gs}\ is\ constant$ …… (5.3.1)

The final expression of drain conductance is written as

$$g_d = \frac{qZ\mu aN_d}{L}\left[1 - \frac{1}{\sqrt{V_p}}\left(V_{bi} - V_{gs} + V_{ds}\right)^{\frac{1}{2}}\right] \text{…… (5.3.2)}$$

Where

$N_d$ = doping concentration

W = Channel width

$V_s$ = carrier Saturation velocity

$R_s$ = parasitic source resistance

$R_d$ = drain resistance

$V_p$ = pinch-off voltage

$V_{bi}$ = Schottky diode built-in voltage

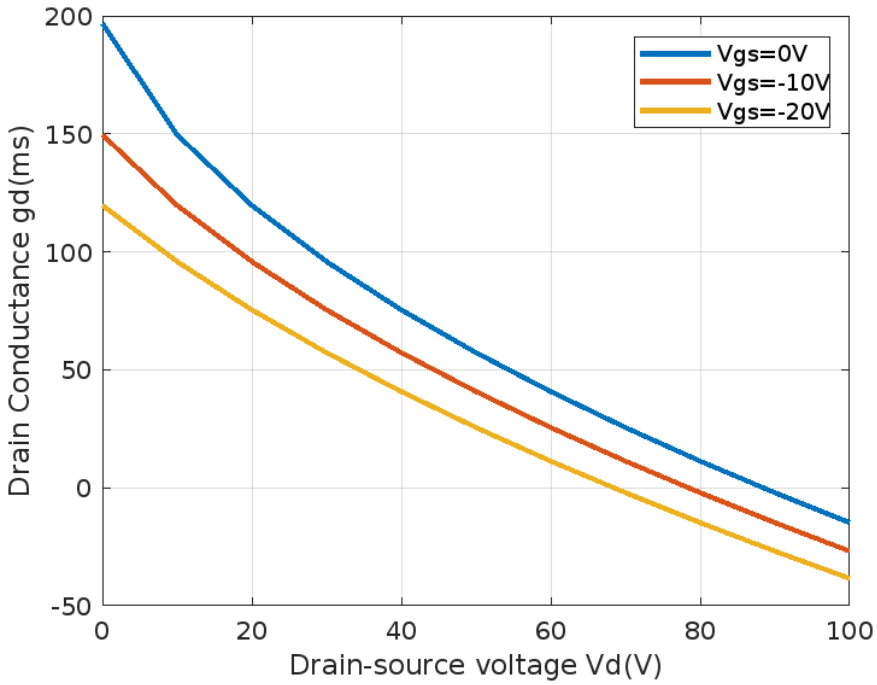


**Figure 6-4the variation of drain conductance (gd) with versus drain-source voltage (Vds)**

MATLAB code used to obtain this plot is given in Chapter-9 MATLAB Code

$N_d = 2x10^{17}cm^{-3}$, channel doping concentration

$N_a = 1x10^{15}cm^{-3}$, substrate doping

$L = 1x10^{-4}cm$, gate- length

$Z = 100x10^{-4}cm$, device width

a = $0.3x10^{-4}cm$. active channel thickness

$W = 2\ X\ 250\ \mu m$Channel width

$R_d = 50\ \Omega$ drain resistance

In figure 5.3.2 the variation of drain conductance ($g_d$) with drain-source voltage (Vds) for different values of $V_{gs} = 0V, -10V, -20V$ .

The $g_d$ values for $V_{gs}$ are exponentially dropped for the $V_{ds}$ of up to 20V. The drain-source voltage in range of 20V to 100V the linear variation of drain-conductance is observed.

There is no significant change of $g_d$ is observed at high drain-source voltage.

## 6.4 Gate-drain capacitance

The parasitic capacitance as defined by [5] is the ability to store charge due to different voltage levels of two electronic components in close proximity to each other. This is an undesired formation of capacitance which is intended to be kept as minimum as possible for it impedes the normal movement of carrier through the channel of MESFET [11].

$$C_{gd} = \frac{ZL}{2\sqrt{2}} \left( \frac{q\varepsilon_s N_d}{V_{bi} - (V_{gs} - V_{ds})} \right)^{\frac{1}{2}} + \frac{\pi}{2} \varepsilon_s Z \ldots\ldots\ldots\ldots\ldots\ldots (5.4.1)$$

Drain capacitance is proportional to the gate length.

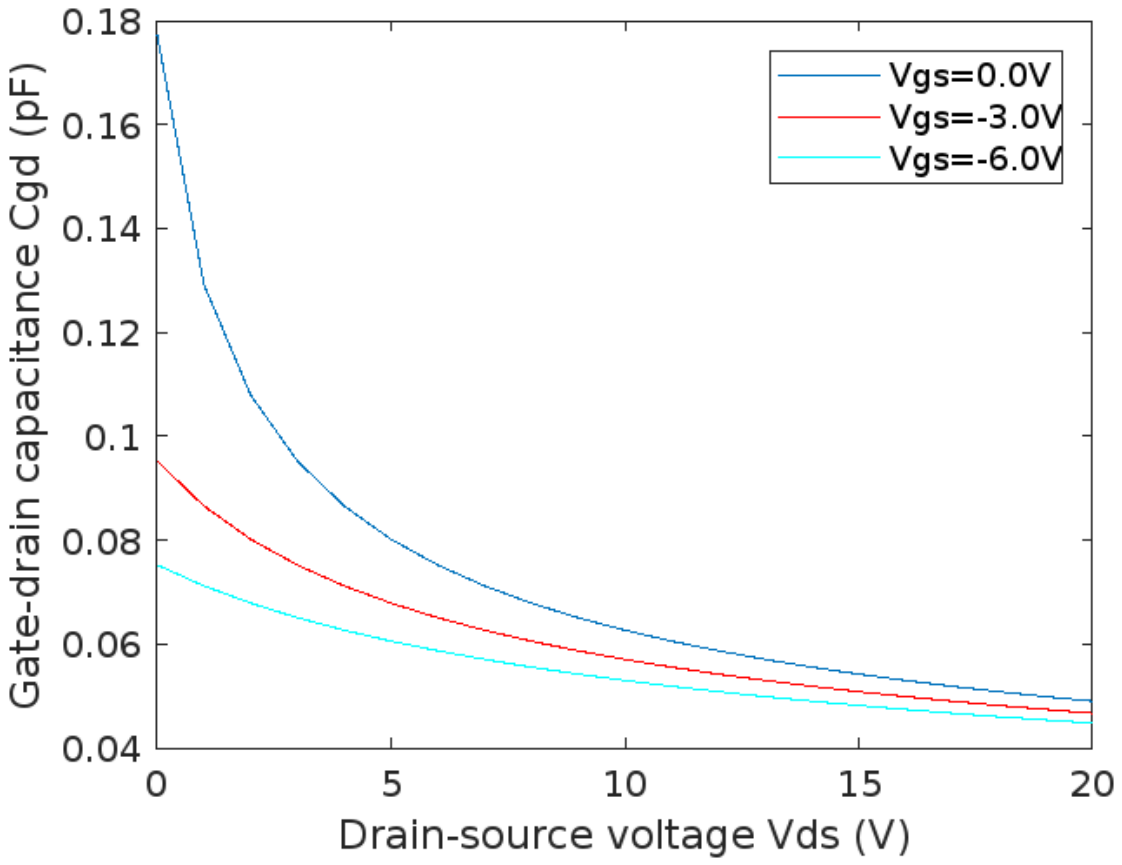


**Figure 6-5 Gate-Drain Capacitance Variation with Drain-Source Voltage for different Gate-Source Voltage**

$N_d = 1x10^{18} cm^{-3}$, channel doping concentration

$N_a = 1x10^{15} cm^{-3}$, substrate doping

$L = 1x10^{-4}cm$, gate- length

$Z = 100x10^{-4}cm$, device width

a = $0.3x10^{-4}cm$. active channel thickness

From the figure it is observed that gate drain conductance decreases with increasing the drain source voltage.at a particular Vds gate drain capacitance less when Vgs is more negative biased.

## 6.5 Gate-source capacitance

$$C_{gs} = \frac{ZL}{2\sqrt{2}}\left(\frac{q\varepsilon N_d}{V_{bi} - V_{gs}}\right)^{\frac{1}{2}} + \frac{\pi}{2}\varepsilon_s Z \quad \ldots\ldots\ldots\ldots\ldots\ldots (5.5.1)$$

From the equation (5.5.1) is is seen that gate source capacitance is directly proportional to L

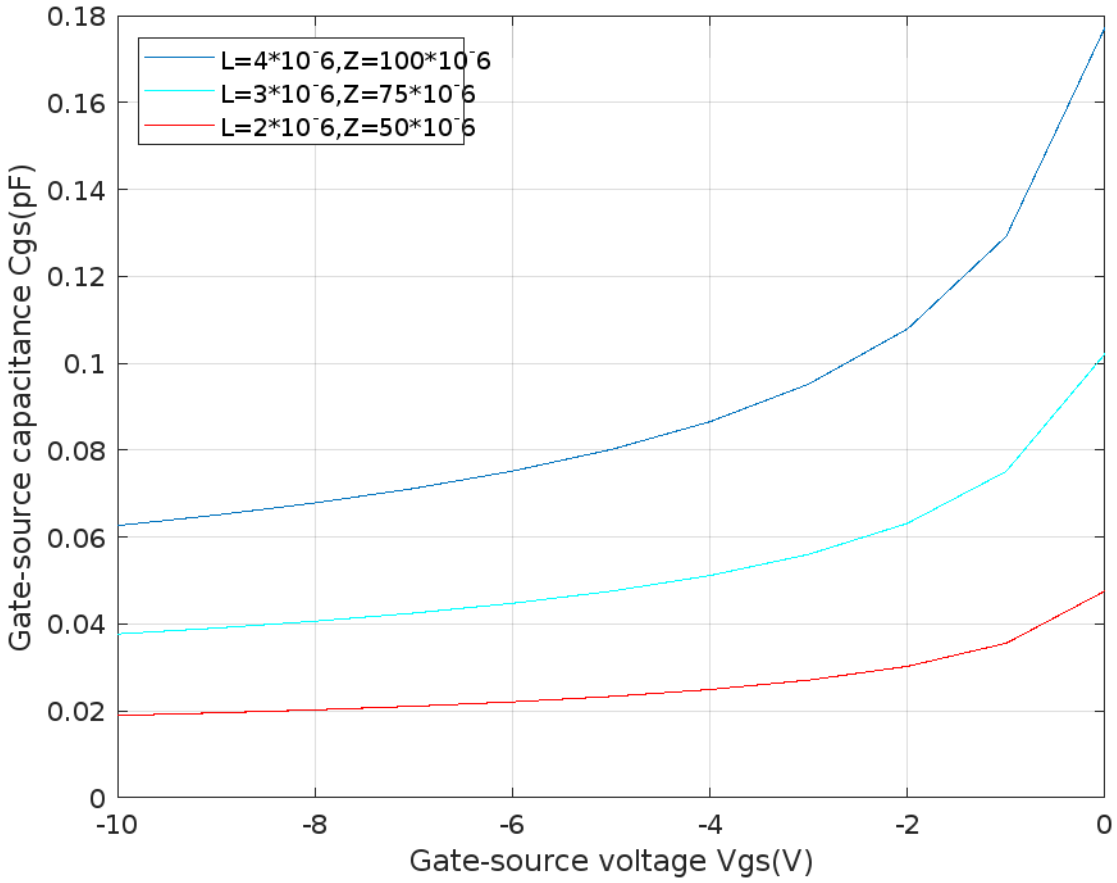


**Figure 6-6 Variation of gate-source capacitance with gate-source voltage**

The value of Cgs is decrease as L decreases from 4µm to 2µm. From Figure 5.5.1 we can see that Cgs has decreased.

## 6.6 Total internal device capacitance

$$C_t = C_{gd} + C_{gs} \ldots\ldots\ldots\ldots\ldots\ldots\ldots (4.30)$$

Following figure 5.6.1 is obtained after executing the MATLAB as given in Chapter - 9

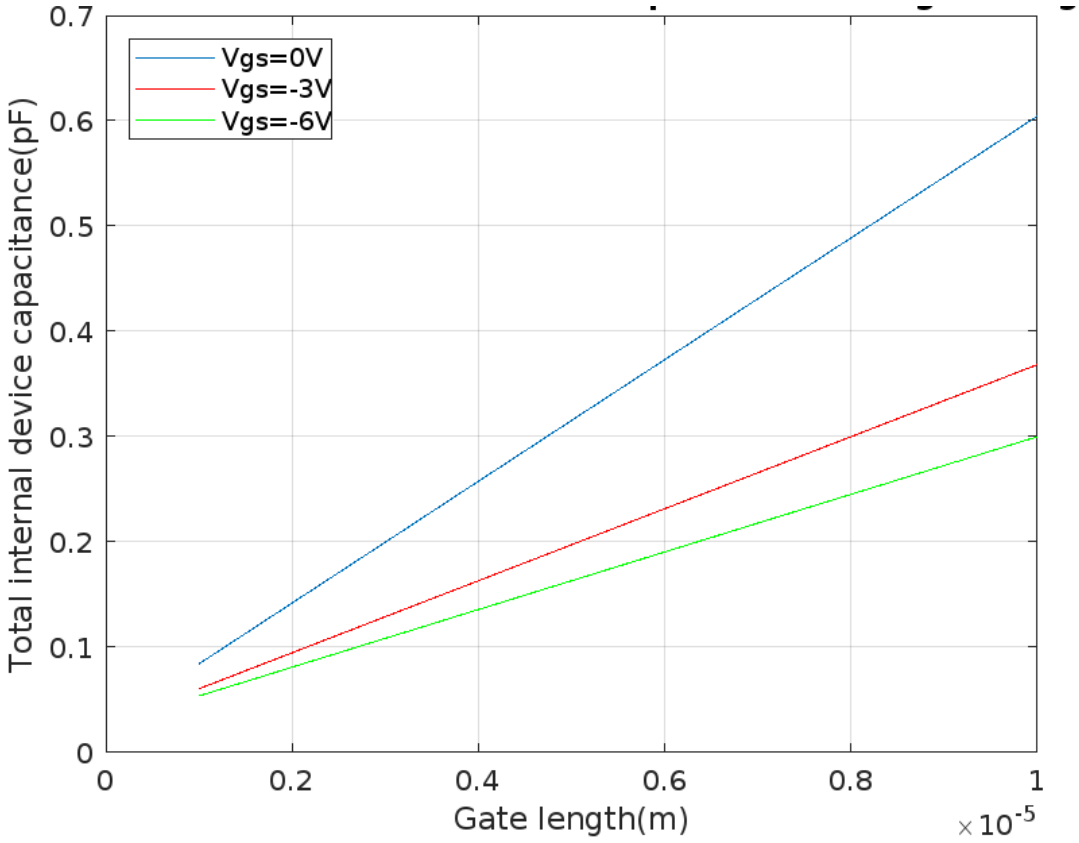


**Figure 6-7 Variation of total internal device capacitance with gate length**

It is seen from the figure that the total internal capacitance is increase with increase of gate length. It is also observed that both Cgs and Cgd are directly proportional to the gate length.

# Chapter 7: Conclusion

In this study we have developed an analytical model to calculate the I-V characteristics MESFET which considers the one-dimensional analysis of the charge distribution in the active region and incorporates the effect of temperature on field electron mobility, velocity saturation and effect of this parameter to the temperature expressions. Moreover, comparisons between the analytical models with different values of temperature showed the effect the output characteristics (I-V) of MESFET,

The variation of transconductance with gate-source voltage shows there is a linear increase in the transconductance with increase in gate-source voltage, and for a fixed drain-source voltage the MESFET with lowest parasitic resistance gives the highest transconductance.

The internal capacitance is seen to increase with increasing gate length and the highest value is obtained with the least negative gate-source voltage.

The parameters have shown the desired trends with variation and can be said to have good agreement with the expected results.

# Chapter 8: Suggestions for Further Work

An analytical two-dimensional channel potential distribution model based on the Poisson's equation is presented in this thesis assuming long-channel MESFET. This potential distribution model can be extended for short-channel MESFETs with some assumptions and modifications. Other practical parameters can be taken into consideration and the effect of gate length modulation and parasitic resistance observed which might help to make a more accurate conclusion about the variation of these parameters and their respective effect on the power and frequency output of GaN MESFET. The possible parameters are Cut-off frequency, Transit time and RC time constant, Maximum Power Density

# Chapter 9: MATLAB Code

## 9.1 Variation of mobility $\mu_1$ with Electric field for different values of temperature

```
u0=3740;
vs=.971;
Ec=0.65e6;
E=0:0.5e5:15e5;


T=100;
%  u1=(u0+vs.*((E.^3)./(Ec.^4)))./(1+(E./Ec).^4);
 u1=(3740.*(T./300).^0.6+vs.*((E.^3)./(Ec.^4)))./(1+(E./Ec).^4);
% u1=3740.*(T./300).^0.6./(1+(E./Ec));

plot(E,u1,'r');
xlabel('Electric Field E (V/m)');
ylabel('Mobility µ1 ( m^2/V.s ');
%title('Mobility with Electric Field');
grid on;
hold on

T=150;
u1=(3740.*(T./300).^0.6+vs.*((E.^3)./(Ec.^4)))./(1+(E./Ec).^4);
plot(E,u1,'g');

T=200;
u1=(3740.*(T./300).^0.6+vs.*((E.^3)./(Ec.^4)))./(1+(E./Ec).^4);
plot(E,u1,'b');

T=250;
u1=(3740.*(T./300).^0.6+vs.*((E.^3)./(Ec.^4)))./(1+(E./Ec).^4);
plot(E,u1,'y');

T=300;
u1=(3740.*(T./300).^0.6+vs.*((E.^3)./(Ec.^4)))./(1+(E./Ec).^4);
plot(E,u1,'c');
legend({'T=100K','T=150K','T=200K','T=250K','T=300K'},'Location','northeast')
grid on
```

## 9.2 Variation of mobility $\mu_2$ with Electric field for different values of temperature

```
u0=3740;
vs=.971;
Ec=0.65e6;
E=0:0.5e5:15e5;
T=100;
u2=((Ec.*3740.*(T./300).^0.6)./E).*tanh(E./Ec);

plot(E,u2,'r');

xlabel('Electric Field E (V/m)');
ylabel('Mobility μ2 ( m^2/N.s ');
%title('Mobility with Electric Field');


hold on;
T=150;
u2=((Ec.*3740.*(T./300).^0.6)./E).*tanh(E./Ec);

plot(E,u2,'g');

T=200;
u2=((Ec.*3740.*(T./300).^0.6)./E).*tanh(E./Ec);

plot(E,u2,'b')

T=250;
u2=((Ec.*3740.*(T./300).^0.6)./E).*tanh(E./Ec);

plot(E,u2,'y')

T=300;
u2=((Ec.*3740.*(T./300).^0.6)./E).*tanh(E./Ec);

plot(E,u2,'c')

legend({'T=100K','T=150K','T=200K','T=250K','T=300K'},'Location','northeast')
grid on
```

## 9.3 Variation of mobility μ_n with Electric field for different values of temperature

```
% carrier Mobility for GaAs MESFET varies with Applied Electric field
%paper: Effect of Mobility on (I-V) Characteristics of Gaas MESFET M Azizi
%paper: Effect of temperature on (TV) statics characteristics of GaAs Mesfet
u0=.374;
vs=.971;
Ec=0.65e6;
E=0:0.5e5:15e5;

T=100;
un=3740.*(T./300).^0.6./(1+(E./Ec).^2);
```

```
plot(E,un,'r');

xlabel('Electric Field E (V/m)');
ylabel('Mobility μ n ( m^2/N.s ');
%title('Mobility with Electric Field');
grid on;
hold on;


T=150;
un=3740.*(T./300).^0.6./(1+(E./Ec).^2);
plot(E,un,'g');

T=200;
un=3740.*(T./300).^0.6./(1+(E./Ec).^2);
plot(E,un,'b');

T=250;
un=3740.*(T./300).^0.6./(1+(E./Ec).^2);
plot(E,un,'y');


T=300;
un=3740.*(T./300).^0.6./(1+(E./Ec).^2);
plot(E,un,'c');

legend({'T=100K','T=150K','T=200K','T=250K','T=300K'},'Location','northeast')
```

## 9.4 Variation of carrier velocity $v_1$ with Electric field for different values of temperature

```
u0=.374;
vs=.971;
Ec=0.65e6;
E=0:0.5e5:20e5;

T=100;
v1=(3740.*(T./300).^0.6+vs.*((E.^3)./(Ec.^4)))./(1+(E./Ec).^4).*E;
plot(E,v1,'r');


xlabel('Electric Field E (V/m)');
ylabel('Carrier velocity V1 (m/s) ');
%title('velocity with Electric Field');
grid on;
hold on;

T=150;
v1=(3740.*(T./300).^0.6+vs.*((E.^3)./(Ec.^4)))./(1+(E./Ec).^4).*E;
plot(E,v1,'g');

T=200;
v1=(3740.*(T./300).^0.6+vs.*((E.^3)./(Ec.^4)))./(1+(E./Ec).^4).*E;
```

```
plot(E,v1,'b');

T=250;
v1=(3740.*(T./300).^0.6+vs.*((E.^3)./(Ec.^4)))./(1+(E./Ec).^4).*E;
plot(E,v1,'y');

T=300;
v1=(3740.*(T./300).^0.6+vs.*((E.^3)./(Ec.^4)))./(1+(E./Ec).^4).*E;
plot(E,v1,'c');

legend({'T=100K','T=150K','T=200K','T=250K','T=300K'},'Location','northeast');
```

## 9.5 Variation of carrier velocity $v_2$ with Electric field for different values of temperature

```
u0=.374;
vs=.971;
Ec=0.65e6;
E=0:0.5e5:20e5;

T=100;

v2=((Ec.*3740.*(T./300).^0.6)./E).*tanh(E./Ec).*E;
plot(E,v2,'r')


xlabel('Electric Field E (V/m)');
ylabel('Carrier velocity V2 (m/s) ');
%title('velocity with Electric Field');
grid on;

hold on;

T=150;

v2=((Ec.*3740.*(T./300).^0.6)./E).*tanh(E./Ec).*E;
plot(E,v2,'g')


T=200;

v2=((Ec.*3740.*(T./300).^0.6)./E).*tanh(E./Ec).*E;
plot(E,v2,'b')


T=250;

v2=((Ec.*3740.*(T./300).^0.6)./E).*tanh(E./Ec).*E;
plot(E,v2,'y')


T=300;
```

```
v2=((Ec.*3740.*(T./300).^0.6)./E).*tanh(E./Ec).*E;
plot(E,v2,'c')


legend({'T=100K','T=150K','T=200K','T=250K','T=300K'},'Location','southeast');
```

## 9.6 Variation of carrier velocity $v_n$ with Electric field for different values of temperature

```
u0=.374;
vs=.971;
Ec=0.65e6;
E=0:0.5e5:20e5;

T=100;
vn=3740.*(T./300).^0.6./(1+(E./Ec).^2).*E;
plot(E,vn,'r')

xlabel('Electric Field E (V/m)');
ylabel('Carrier velocity vn (m/s) ');
%title('velocity with Electric Field');
grid on;
hold on;

T=150;
vn=3740.*(T./300).^0.6./(1+(E./Ec).^2).*E;
plot(E,vn,'g');

T=200;
vn=3740.*(T./300).^0.6./(1+(E./Ec).^2).*E;
plot(E,vn,'b');

T=250;
vn=3740.*(T./300).^0.6./(1+(E./Ec).^2).*E;
plot(E,vn,'y');

T=300;
vn=3740.*(T./300).^0.6./(1+(E./Ec).^2).*E;
plot(E,vn,'c');

legend({'T=100K','T=150K','T=200K','T=250K','T=300K'},'Location','northeast');
```

## 9.7 Variation of Drain-Source Current with Drain-Source Voltage

```
clc;
clear all;
close all;
%variable
u = 0.15;
```

```
eps = 9.5*8.8542e-12;
max_iter= 100;
tol =.000000001;
a = 7.5*(10^-8);
d = 0.15e-6;
Vp = 16;
%fixed
q = 1.6*(10^-19);
Z = 100*(10^-6);
Nd = 1*(10^23);
L = 4*(10^-6);
Rs = 75;
Rd = 75;
Vbi = 1;
Vgs = 0;
%Vds = 5;
Vds = 0:1:10;
Ids(1) = 0;
for i=1:length(Vds)

    for k = 1:max_iter
Ids (k+1)= ((q*Z*u*Nd*a)/L)*(Vds(i)-Ids(k)*(Rs+Rd)-(2/(3*sqrt(Vp)))*((Vbi-
Vgs+Vds(i)-Ids(k)*Rd)^(3/2)-(Vbi-Vgs+Ids(k)*Rs)^(3/2)));
err = abs((Ids(k+1)-Ids(k))/Ids(k+1));
if(err<tol)
 sol(i) = Ids(k+1);
 break;
 end
end
 sol(i) = (Ids(k+1))*1000;
end
plot (Vds, sol);

ylabel('Drain-source current (mA)');
xlabel('Drain-source voltage(V)');
%title('Ids-Vds characteristicsfor GaN MESFET');

hold on;
Vgs = -3;
Vds = 0:1:10;
Ids(1) = 0;
for i=1:length(Vds)
for k = 1:max_iter
Ids(k+1) = ((q*Z*u*Nd*a)/L)*(Vds(i)-Ids(k)*(Rs+Rd)-(2/(3*(sqrt(Vp))))*((Vbi-
Vgs+Vds(i)-(Ids(k)*Rd))^(3/2)-(Vbi-Vgs+( Ids(k)*Rs))^(3/2)));
 err = abs((Ids(k+1)-Ids(k))/Ids(k+1));
 if(err<tol)
sol(i) = Ids(k+1);
 break;
 end
end

sol(i) = (Ids(k+1))*1000;
end
plot (Vds, sol, 'r')
```

```
hold on;
Vgs = -6;
%Vds = 5;
Vds = 0:1:10;
Ids(1) = 0;
for i=1:length(Vds)
for k = 1:max_iter
Ids(k+1) = ((q*Z*u*Nd*a)/L)*(Vds(i)-Ids(k)*(Rs+Rd)-(2/(3*(sqrt(Vp))))*((Vbi-
Vgs+Vds(i)-(Ids(k)*Rd))^(3/2)-(Vbi-Vgs+( Ids(k)*Rs))^(3/2)));
 err = abs((Ids(k+1)-Ids(k))/Ids(k+1));
 if(err<tol)
 sol(i) = Ids(k+1);
 break;
 end
end
 sol(i) = (Ids(k+1))*1000;
end
plot (Vds, sol, 'g')
% hold on;
% Vgs = -9;
% %Vds = 5;
% Vds = 0:1:10;
% Ids(1) = 0;
% for i=1:length(Vds)
% for k = 1:max_iter
% Ids(k+1) = ((q*Z*u*Nd*a)/L)*(Vds(i)-Ids(k)*(Rs+Rd)-(2/(3*(sqrt(Vp))))*((Vbi-
Vgs+Vds(i)-(Ids(k)*Rd))^(3/2)-(Vbi-Vgs+( Ids(k)*Rs))^(3/2)));
%  err = abs((Ids(k+1)-Ids(k))/Ids(k+1));
%  if(err<tol)
%  sol(i) = Ids(k+1);
%  break;
%  end
% end
%  sol(i) = (Ids(k+1))*1000;
% end
% plot (Vds, sol, 'c')
hold on;
Kd = 1;
Vsat = 0.26*10^4;
Es = Vsat/u;
Vgs = 0;
Vt = Vbi-Vp;
V1s = (Es*L*(Vgs-Vt))/(Es*L+(Vgs-Vt));
eps = 9.5*8.8542*10^-12;
Vds = [10:1:20];
for i = 1:length(Vds)
 Ls(i)=L-((2*a)/pi)*asinh((pi*Kd*(Vds(i)-V1s))/(2*a*Es));
 V2s(i) = Vds(i)-V1s;
 Lsb(i) = ((1-Kd)*V2s(i))/(Es*cosh((pi*Ls(i))/(2*a)));
 B(i)=(2*eps*Vsat*Z)/(a*(Vp+3*Es*Ls(i))) ;
 Idsat(i)= (1+2*B(i)*Rs*(Vgs-Vt)-sqrt(1+4*B(i)*Rs*(Vgs-Vt)))/(2*B(i)*Rs^2);
 Idsatb(i)=(Idsat(i)*(1+(Ls(i)+Lsb(i))/L))*1000;
end
plot(Vds,Idsatb)
hold on;
```

```
Vgs = -3;
Vsat = 0.28*10^4;
Vds = [10:1:20];
for i = 1:length(Vds)
 Ls(i)=L-((2*a)/pi)*asinh((pi*Kd*(Vds(i)-V1s))/(2*a*Es));
 V2s(i) = Vds(i)-V1s;
 Lsb(i) = ((1-Kd)*V2s(i))/(Es*cosh((pi*Ls(i))/(2*a)));
 B(i)=(2*eps*Vsat*Z)/(a*(Vp+3*Es*Ls(i))) ;
 Idsat(i)= (1+2*B(i)*Rs*(Vgs-Vt)-sqrt(1+4*B(i)*Rs*(Vgs-Vt)))/(2*B(i)*Rs^2);
 Idsatb(i)=(Idsat(i)*(1+(Ls(i)+Lsb(i))/L))*1000;
end
plot(Vds,Idsatb,'r')
hold on;
Vgs = -6;
Vsat = 0.29*10^4;
Vds = [10:1:20];
for i = 1:length(Vds)
     Ls(i)=L-((2*a)/pi)*asinh((pi*Kd*(Vds(i)-V1s))/(2*a*Es));
 V2s(i) = Vds(i)-V1s;
 Lsb(i) = ((1-Kd)*V2s(i))/(Es*cosh((pi*Ls(i))/(2*a)));
 B(i)=(2*eps*Vsat*Z)/(a*(Vp+3*Es*Ls(i))) ;
 Idsat(i)= (1+2*B(i)*Rs*(Vgs-Vt)-sqrt(1+4*B(i)*Rs*(Vgs-Vt)))/(2*B(i)*Rs^2);
 Idsatb(i)=(Idsat(i)*(1+(Ls(i)+Lsb(i))/L))*1000;
end
plot(Vds,Idsatb,'g')
%{
hold on;
Vgs = -9;
Vsat = 0.19*10^4;
Vds = 10:1:20;
for i = 1:length(Vds)
 Ls(i)=L-((2*a)/pi)*asinh((pi*Kd*(Vds(i)-V1s))/(2*a*Es));
 V2s(i) = Vds(i)-V1s;
 Lsb(i) = ((1-Kd)*V2s(i))/(Es*cosh((pi*Ls(i))/(2*a)));
 B(i)=(2*eps*Vsat*Z)/(a*(Vp+3*Es*Ls(i))) ;
 Idsat(i)= (1+2*B(i)*Rs*(Vgs-Vt)-sqrt(1+4*B(i)*Rs*(Vgs-Vt)))/(2*B(i)*Rs^2);
 Idsatb(i)=(Idsat(i)*(1+(Ls(i)+Lsb(i))/L))*1000;
end
plot(Vds,Idsatb,'c')
%}
%{
text(10,2.5,'Vgs=-9V')
text(10,6,'Vgs=-6V')
text(10,10,'Vgs=-3V')
text(10,14,'Vgs=-0V')
%}
legend({'Vgs=0.0V','Vgs=-3.0V','Vgs=-6.0V',},'Location','southeast')
grid on;
```

## 9.8 Variation of Transconductance with Gate-Source Voltage

```
clc;
close all;
clear all;
```

```
a = 7.5*(10^-8);
Kd = 0.6;
Vsat = 0.27*10^4;
u = 0.15;
Es = Vsat/u;
L = 4*(10^-6);
Vbi = 1;
Vp = 16;
Vt = Vbi-Vp;
eps = 9.5*8.8542*10^-12;
Rs = 75;
Z = 100*(10^-6);
Vds = 10;
gm = zeros(1,10);
syms Vgs
gyb=diff((((1+2*((2*eps*Vsat*Z)/(a*(Vp+3*Es*(L-((2*a)/pi)*asinh((pi*Kd*(Vds-
((Es*L*(Vgs-Vt))/(Es*L+(Vgs-Vt)))))/(2*a*Es))))) )*Rs*(Vgs-Vt)-
sqrt(1+4*((2*eps*Vsat*Z)/(a*(Vp+3*Es*(L-((2*a)/pi)*asinh((pi*Kd*(Vds-((Es*L*(Vgs-
Vt))/(Es*L+(Vgs-Vt)))))/(2*a*Es))))) )*Rs*(Vgs-
Vt)))/(2*((2*eps*Vsat*Z)/(a*(Vp+3*Es*(L-((2*a)/pi)*asinh((pi*Kd*(Vds-((Es*L*(Vgs-
Vt))/(Es*L+(Vgs-Vt)))))/(2*a*Es))))) )*Rs^2))*(1+((L-((2*a)/pi)*asinh((pi*Kd*(Vds-
((Es*L*(Vgs-Vt))/(Es*L+(Vgs-Vt)))))/(2*a*Es)))+(((1-Kd)*(Vds-((Es*L*(Vgs-
Vt))/(Es*L+(Vgs-Vt)))))/(Es*cosh((pi*(L-((2*a)/pi)*asinh((pi*Kd*(Vds-((Es*L*(Vgs-
Vt))/(Es*L+(Vgs-Vt)))))/(2*a*Es))))/(2*a)))))/L)));
gy = gyb/(1+gyb*Rs);
gm(1)=(subs(gy,Vgs,-9))*1000/(Z*10^3);

gm(2)=(subs(gy,Vgs,-8))*1000/(Z*10^3);
gm(3)=(subs(gy,Vgs,-7))*1000/(Z*10^3);
gm(4)=(subs(gy,Vgs,-6))*1000/(Z*10^3);
gm(5)=(subs(gy,Vgs,-5))*1000/(Z*10^3);
gm(6)=(subs(gy,Vgs,-4))*1000/(Z*10^3);
gm(7)=(subs(gy,Vgs,-3))*1000/(Z*10^3);
gm(8)=(subs(gy,Vgs,-2))*1000/(Z*10^3);
gm(9)=(subs(gy,Vgs,-1))*1000/(Z*10^3);
gm(10)=(subs(gy,Vgs,0))*1000/(Z*10^3);
Vgs = [-9:1:0];
plot(Vgs,gm),xlabel('Gate-source voltage(V)'),ylabel('Transconductance(ms/mm)');
%title('Variation of transconductance with gate-source voltage')
hold on;
Vsat = 0.28*10^4;
Vds = 12;
gm = zeros(1,10);
syms Vgs
gyb=diff((((1+2*((2*eps*Vsat*Z)/(a*(Vp+3*Es*(L-((2*a)/pi)*asinh((pi*Kd*(Vds-
((Es*L*(Vgs-Vt))/(Es*L+(Vgs-Vt)))))/(2*a*Es))))) )*Rs*(Vgs-Vt)-
sqrt(1+4*((2*eps*Vsat*Z)/(a*(Vp+3*Es*(L-((2*a)/pi)*asinh((pi*Kd*(Vds-((Es*L*(Vgs-
Vt))/(Es*L+(Vgs-Vt)))))/(2*a*Es))))) )*Rs*(Vgs-
Vt)))/(2*((2*eps*Vsat*Z)/(a*(Vp+3*Es*(L-((2*a)/pi)*asinh((pi*Kd*(Vds-((Es*L*(Vgs-
Vt))/(Es*L+(Vgs-Vt)))))/(2*a*Es))))) )*Rs^2))*(1+((L-((2*a)/pi)*asinh((pi*Kd*(Vds-
((Es*L*(Vgs-Vt))/(Es*L+(Vgs-Vt)))))/(2*a*Es)))+(((1-Kd)*(Vds-((Es*L*(Vgs-
Vt))/(Es*L+(Vgs-Vt)))))/(Es*cosh((pi*(L-((2*a)/pi)*asinh((pi*Kd*(Vds-((Es*L*(Vgs-
Vt))/(Es*L+(Vgs-Vt)))))/(2*a*Es))))/(2*a)))))/L)));
gy = gyb/(1+gyb*Rs);
gm(1)=(subs(gy,Vgs,-9))*1000/(Z*10^3);
```

```
gm(2)=(subs(gy,Vgs,-8))*1000/(Z*10^3);
gm(3)=(subs(gy,Vgs,-7))*1000/(Z*10^3);
gm(4)=(subs(gy,Vgs,-6))*1000/(Z*10^3);

gm(5)=(subs(gy,Vgs,-5))*1000/(Z*10^3);
gm(6)=(subs(gy,Vgs,-4))*1000/(Z*10^3);
gm(7)=(subs(gy,Vgs,-3))*1000/(Z*10^3);
gm(8)=(subs(gy,Vgs,-2))*1000/(Z*10^3);
gm(9)=(subs(gy,Vgs,-1))*1000/(Z*10^3);
gm(10)=(subs(gy,Vgs,0))*1000/(Z*10^3);
Vgs = [-9:1:0];
plot(Vgs,gm,'r')
hold on;
Vsat = 0.29*10^4;
Vds = 15;
gm = zeros(1,10);
syms Vgs
gyb=diff((((1+2*((2*eps*Vsat*Z)/(a*(Vp+3*Es*(L-((2*a)/pi)*asinh((pi*Kd*(Vds-
((Es*L*(Vgs-Vt))/(Es*L+(Vgs-Vt)))))/(2*a*Es))))) )*Rs*(Vgs-Vt)-
sqrt(1+4*((2*eps*Vsat*Z)/(a*(Vp+3*Es*(L-((2*a)/pi)*asinh((pi*Kd*(Vds-((Es*L*(Vgs-
Vt))/(Es*L+(Vgs-Vt)))))/(2*a*Es))))) )*Rs*(Vgs-
Vt)))/(2*((2*eps*Vsat*Z)/(a*(Vp+3*Es*(L-((2*a)/pi)*asinh((pi*Kd*(Vds-((Es*L*(Vgs-
Vt))/(Es*L+(Vgs-Vt)))))/(2*a*Es))))) )*Rs^2))*(1+((L-((2*a)/pi)*asinh((pi*Kd*(Vds-
((Es*L*(Vgs-Vt))/(Es*L+(Vgs-Vt)))))/(2*a*Es)))+(((1-Kd)*(Vds-((Es*L*(Vgs-
Vt))/(Es*L+(Vgs-Vt)))))/(Es*cosh((pi*(L-((2*a)/pi)*asinh((pi*Kd*(Vds-((Es*L*(Vgs-
Vt))/(Es*L+(Vgs-Vt)))))/(2*a*Es))))/(2*a)))))/L)));
gy = gyb/(1+gyb*Rs);
gm(1)=(subs(gy,Vgs,-9))*1000/(Z*10^3);
gm(2)=(subs(gy,Vgs,-8))*1000/(Z*10^3);
gm(3)=(subs(gy,Vgs,-7))*1000/(Z*10^3);
gm(4)=(subs(gy,Vgs,-6))*1000/(Z*10^3);
gm(5)=(subs(gy,Vgs,-5))*1000/(Z*10^3);
gm(6)=(subs(gy,Vgs,-4))*1000/(Z*10^3);
gm(7)=(subs(gy,Vgs,-3))*1000/(Z*10^3);

gm(8)=(subs(gy,Vgs,-2))*1000/(Z*10^3);
gm(9)=(subs(gy,Vgs,-1))*1000/(Z*10^3);
gm(10)=(subs(gy,Vgs,0))*1000/(Z*10^3);
Vgs = [-9:1:0];
plot(Vgs,gm,'Color','g');
grid on;

legend({'Vds=10V','Vds=12V','Vds=15V',},'Location','southeast');
```

## 9.9 Variation of Drain conductance with Gate-Source Voltage

```
clc;
clear all;
close all;
q = 1.6e-19;
K = 1.3807e-23;
e = 8.854e-14;
epsilon = 8.9*e;
Nd = 1e18;
```

```
Na= 1e15;
a = 0.3e-4;
L = 1e-4;
u = 500;
z = 100e-4;
To=300;
Eg = 3.23;
Nc = 3.25e14*sqrt(To*To*To);
Nv = 4.8e15*sqrt(To*To*To);
ni = sqrt(Nc*Nv)*exp(-(Eg*q)/(2*K*To));
Vbi = (0.0259)*(log((Nd*Na)/(ni*ni)));
Vds = [0 10 20 30 40 50 60 70 80 90 100];
Vgs = [0 -10 -20];
for i=1:3
for j=1:11
a1 = (q*z*u*a*Nd)/L;
Vp = ((q*Nd*a*a)/(2*epsilon));
a2(i,j) = (Vbi-Vgs(i)+Vds(j))^(1/2);
a3(i) = (Vp)^(1/2);
a4(i,j)=(a2(i,j)/a3(i));
gd(i,j) = a1*(1-(a4(i,j)));
end
end
plot(Vds,gd*1000,'LineWidth',2.0);
xlabel('Drain-source voltage Vd(V)');
ylabel('Drain Conductance gd(ms)');
%title('Drain Conductance Vs Drain Voltage');
grid on;

legend({'Vgs=0V','Vgs=-10V','Vgs=-20V',},'Location','northeast');
```

## 9.10 Variation of Gate-Source Capacitance with respect to Gate-Source Voltage

```
clear all;
clc;
close all;
%Z = 100*10^-6;
%L = 4*10^-6;
q = 1.6*10^-19;
Eo = 8.85*10^-12;
E = 9.5*Eo;
Nd = 10^23;
Vbi = 1;
Vgs = [-10:1:0];
L = 4*10^-6;
Z = 100*10^-6;
Cgs = (((Z*L)./(2*2^0.5)).*sqrt((q*E*Nd)./(Vbi-Vgs)) + (pi./2)*E*Z)*10^12;
plot(Vgs,Cgs), xlabel('Gate-source voltage Vgs(V)'),ylabel('Gate-source capacitance
Cgs(pF)');
%title('Variation of gate-source capacitance with gate-source voltage')
```

```
hold on;
L = 3*10^-6;
Z = 75*10^-6;
Cgs = (((Z*L)./(2*2^0.5)).*sqrt((q*E*Nd)./(Vbi-Vgs)) + (pi./2)*E*Z)*10^12;
plot(Vgs,Cgs,'c');


hold on;
L = 2*10^-6;
Z = 50*10^-6;
Cgs = (((Z*L)./(2*2^0.5)).*sqrt((q*E*Nd)./(Vbi-Vgs)) + (pi./2)*E*Z)*10^12;
plot(Vgs,Cgs,'r');

legend({'L=4*10^-6,Z=100*10^-6','L=3*10^-6,Z=75*10^-6','L=2*10^-6,Z=50*10^-
6','L=1*10^-6,Z=25*10^-6'},'Location','northwest');
grid on;
```

## 9.11 Variation of Gate-Drain Capacitance with Drain-Source Voltage

```
clear all;
clc;
close all;
Z = 100*10^-6;
L = 4*10^-6;
q = 1.6*10^-19;
Eo = 8.85*10^-12;
E = 9.5*Eo;
Nd = 10^23;
Vbi = 1;
Vds = [0:1:20];
Vgs = 0;
Cgd = (((Z*L)./(2*2^0.5)).*sqrt((q*E*Nd)./(Vbi-(Vgs-Vds))) + (pi./2)*E*Z)*10^12;
plot(Vds,Cgd), xlabel('Drain-source voltage Vds (V)'),ylabel('Gate-drain
capacitance Cgd (pF)');
% title('Variation of gate-drain capacitance with drain-source voltages')
hold on;
Vgs = -3;
Cgd = (((Z*L)./(2*2^0.5)).*sqrt((q*E*Nd)./(Vbi-(Vgs-Vds))) + (pi./2)*E*Z)*10^12;
plot(Vds,Cgd,'r')
hold on;
Vgs = -6;
Cgd = (((Z*L)./(2*2^0.5)).*sqrt((q*E*Nd)./(Vbi-(Vgs-Vds))) + (pi./2)*E*Z)*10^12;
plot(Vds,Cgd,'c')

legend({'Vgs=0.0V','Vgs=-3.0V','Vgs=-6.0V'},'Location','northeast')
```

## 9.12 Variation of Total Internal Device Capacitance with Gate Length

```
clc;
close all;
clear all;
Z=100*10^-6;
q=1.6022*10^-19;
```

```
eps=9.5*8.854*10^-12;
Nd=1*10^23;
Vbi=1;
Vds=5;
Vgs=0;
L = [1*(10^-6):1*(10^-6):10*(10^-6)];
for i = 1:length(L)
 Cgs = ((Z*L/(2*sqrt(2)))*(sqrt(q*eps*Nd/(Vbi-Vgs)))+ (pi*eps*Z)/2)*10^12;
 Cgd = ((Z*L/(2*sqrt(2)))*(sqrt(q*eps*Nd/(Vbi-(Vgs-Vds))))+ (pi*eps*Z)/2)*10^12;
end
Ct = Cgs+Cgd;
plot(L,Ct),xlabel('Gate length(m)'),ylabel('Total internal device
capacitance(pF)'), title('Variation of total internal device capacitance with gate
length')
hold on;
Vgs=-3;
L = [1*(10^-6):1*(10^-6):10*(10^-6)];
for i = 1:length(L)
 Cgs = ((Z*L/(2*sqrt(2)))*(sqrt(q*eps*Nd/(Vbi-Vgs)))+ (pi*eps*Z)/2)*10^12;
 Cgd = ((Z*L/(2*sqrt(2)))*(sqrt(q*eps*Nd/(Vbi-(Vgs-Vds))))+ (pi*eps*Z)/2)*10^12;

end
Ct = Cgs+Cgd;
plot(L,Ct,'r');
hold on;
 Vgs=-6;
L = [1*(10^-6):1*(10^-6):10*(10^-6)];
for i = 1:length(L)
 Cgs = ((Z*L/(2*sqrt(2)))*(sqrt(q*eps*Nd/(Vbi-Vgs)))+ (pi*eps*Z)/2)*10^12;
 Cgd = ((Z*L/(2*sqrt(2)))*(sqrt(q*eps*Nd/(Vbi-(Vgs-Vds))))+ (pi*eps*Z)/2)*10^12;
 end
Ct = Cgs+Cgd;
plot(L,Ct,'g');
legend({'Vgs=0V','Vgs=-3V','Vgs=-6V'},'Location','northwest')
grid on
```

# Chapter 10: Reference


[1] Effect of Mobility on (I-V) Characteristics of Gaas MESFETM Azizi, C AziziFaculty of exact sciences and natural and life sciences, Active Devices and Materials Laboratory, Larbi Ben M'Hidi University, Oum El Bouaghi, Algéria

[2] Effect of temperature on (IV) statics characteristics of GaAs Mesfet Z. Fares (1), Y. Saidi

[3] Analysis of Temperature Effect on MOSFET Parameter using MATLAB 1Jitty Jose, 2Keerthi K Nair, 3Ajith Ravindran

[4] Temperature dependent analytical model for submicron GaAs-MESFET, **Mohamed Djouder, Arezki Benfdila, Ahcene Lakhlef**

[5] The Influence of Electric Field and Mobility Profile on GaAs MESFET Characteristics, CHUNG-SHU

[6] http://epcco.com/epc/documents/producttraining/Appnote_GaNfundamentals.pdf

[7] Chapter-3, GaN material technology - http://itri2.org/ttec/hte_j/report/03.pdf

[8] http://en.wikipedia.org/wiki/Band_gap

[9] http://en.wikipedia.org/wiki/Electron_mobility

[10] http://en.wikipedia.org/wiki/Saturation_velocity

[11] http://en.wikipedia.org/wiki/Thermal_conductivity

[12] GaN vs SiC - http://www.digikey.com/Web%20Export/Supplier%20Content/ Microsemi_278/PDF/Microsemi_GalliumNitride_VS_SiliconCarb ide.pdf?redirected=

[13] Azam, Sher (Linköping University, Department of Physics, Chemistry and Biology, Materials Science ) (Linköping University, The Institute of Technology), Linköping Studies in Science and Technology. Thesis, ISSN 0280-7971; 1374, "Wide Bandgap Semiconductor (SiC & GaN) Power Amplifiers in Different Classes".

[14] Potential Performance of SiC and GaN Based Metal Semiconductor Field Effect transistorsH. Arabshahi Department of Physics, Ferdowsi University of Mashhad, P.O. Box 91775-1436, Mashhad, Iran (Received on 23 July, 2008).

[15] Pulsed measurements of GaN MESFETs B. Boudart, S. Trassaert, C. Gaquiere, D. Theron and Y. Crosner Institut d'Electronique et de Microelectronique du Nord – DHS U.M.R. - C.N.R.S. 8520- USTL – Avenue Poincare- B.P. 69 59652 VILLENEUVE D'ASCQ CEDEX – France.

[16] Investigation of cross sectional potential distributionM.Kaneko, A.Hinoki, A.Suzuki, T.Araki,Y.Nanishi

[17] Double-ion-implanted GaN MESFETs with extremely low source/drain resistance74

[18] A complete analytical model of GaN MESFET for microwave frequency applications -

[19] S.Bose, Adarsh, A.Kumar, Simrata, M.Gupta, R.S. Gupta, Received 11 April 2001; revised 23 May 2001; accepted 4 June 2001.